

**Systematic  
investigation of BrO  
in volcanic plumes  
with GOME-2**

C. Hörmann et al.

This discussion paper is/has been under review for the journal Atmospheric Chemistry and Physics (ACP). Please refer to the corresponding final paper in ACP if available.

# Systematic investigation of bromine monoxide in volcanic plumes from space by using the GOME-2 instrument

**C. Hörmann<sup>1,2</sup>, H. Sihler<sup>1,2</sup>, N. Bobrowski<sup>2</sup>, S. Beirle<sup>1</sup>, M. Penning de Vries<sup>1</sup>, U. Platt<sup>2</sup>, and T. Wagner<sup>1</sup>**

<sup>1</sup>Max-Planck-Institute for Chemistry, Mainz, Germany

<sup>2</sup>Institute for Environmental Physics, University of Heidelberg, Germany

Received: 12 September 2012 – Accepted: 6 November 2012 – Published: 15 November 2012

Correspondence to: C. Hörmann (c.hoermann@mpic.de)

Published by Copernicus Publications on behalf of the European Geosciences Union.

Title Page

Abstract

Introduction

Conclusions

References

Tables

Figures

⏪

⏩

◀

▶

Back

Close

Full Screen / Esc

Printer-friendly Version

Interactive Discussion

## Abstract

During recent years, volcanic emissions turned out to be a natural source of bromine compounds in the atmosphere. While the initial formation process of bromine monoxide (BrO) has been successfully studied in local ground-based measurements at quiescent degassing volcanoes worldwide, literature on the chemical evolution of BrO on large spatial and temporal scales is sparse. The first space-based observation of a volcanic BrO plume following the Kasatochi eruption in 2008 demonstrated the capability of satellite instruments to monitor such events on a global scale.

In this study, we systematically examined GOME-2 observations from January 2007 until June 2011 for significantly enhanced BrO slant column densities (SCDs) in the vicinity of volcanic plumes. In total, 772 plumes from at least 37 volcanoes have been found by using sulphur dioxide (SO<sub>2</sub>) as a tracer for a volcanic plume. All captured SO<sub>2</sub> plumes were subsequently analysed for a simultaneous enhancement of BrO and the data were checked for a possible spatial correlation between the two species. Additionally, the mean BrO/SO<sub>2</sub> ratios for all volcanic plumes have been calculated by the application of a bivariate linear fit.

A total number of 64 volcanic plumes from at least 11 different volcanoes showed clear evidence for BrO of volcanic origin, revealing large differences in the BrO/SO<sub>2</sub> ratios (ranging from some 10<sup>-5</sup> to several 10<sup>-4</sup>) and the spatial distribution of both species. A close correlation between SO<sub>2</sub> and BrO occurred only for some of the observed eruptions or just in certain parts of the examined plumes. For other cases, only a rough spatial relationship was found. We discuss possible explanations for the occurrence of the different spatial SO<sub>2</sub> and BrO distributions in aged volcanic plumes.

## 1 Introduction

BrO is an important catalyst in the depletion of ozone (O<sub>3</sub>) in the stratosphere and troposphere, especially during springtime in polar regions (see Barrie et al., 1988;

ACPD

12, 29325–29389, 2012

## Systematic investigation of BrO in volcanic plumes with GOME-2

C. Hörmann et al.

Title Page

Abstract

Introduction

Conclusions

References

Tables

Figures

⏪

⏩

◀

▶

Back

Close

Full Screen / Esc

Printer-friendly Version

Interactive Discussion



Simpson et al., 2007, and references therein). In addition to sources like the surfaces of salt lakes, polar sea ice or sea-salt aerosol in the mid-latitude marine boundary layer (von Glasow and Crutzen, 2003), volcanic emissions turned out to be a further natural source of bromine compounds and the subsequent formation of BrO (Bobrowski et al., 2003). The injection of BrO that has formed in volcanic plumes is, therefore, very likely to have a significant impact on atmospheric chemistry (von Glasow, 2010).

BrO in a volcanic plume was detected for the first time by Bobrowski et al. (2003), using ground-based Multi-Axis Differential Optical Absorption Spectroscopy (MAX-DOAS) measurements at the Soufrière Hills volcano on Montserrat. The BrO slant column densities (SCDs) were found to be closely correlated to the measured SO<sub>2</sub> SCDs, resulting in an average BrO/SO<sub>2</sub> molar ratio of  $\sim 8.2 \times 10^{-4}$  (equal to a Br/S mass ratio of  $\sim 2 \times 10^{-3}$ ). Based on this ratio, the authors estimated a global emission of 30 000 t Br yr<sup>-1</sup> using the estimation of the global volcanic SO<sub>2</sub>-source-strength of about  $14 \pm 6$  Tg SO<sub>2</sub> yr<sup>-1</sup> by Graf et al. (1997). Since then, similar ground-based observations were made at several volcanoes worldwide (e.g. Galle et al., 2005; Oppenheimer et al., 2006; Bobrowski and Platt, 2007; Boichu et al., 2011, and references therein). All these measurements revealed an almost linear correlation between the two species and typical BrO/SO<sub>2</sub> molar ratios ranging from  $1 \times 10^{-5}$  to  $8.2 \times 10^{-4}$ . In addition to the ground-based measurements, BrO has also been detected by airborne observations of volcanic plumes during the recent years (e.g. Bani et al., 2009; Heue et al., 2011; Kelly et al., 2012).

First considerations about the origin of BrO in volcanic plumes in Bobrowski et al. (2003) and Gerlach (2004) suggested that BrO is probably not directly emitted by volcanoes, but formed as a secondary product from near-vent, high-temperature oxidation of magmatic gases and heterogeneous chemistry involving sulphate aerosols inside the plume. Motivated by that suggestion, Oppenheimer et al. (2006) and Bobrowski et al. (2007) investigated the daytime plume of Mt. Etna (Sicily) at different distances, directly at the summit crater, but also further away at a plume age of a few minutes. As BrO was only observed in the downwind plume (not in the crater measurements), these

**Systematic investigation of BrO in volcanic plumes with GOME-2**

C. Hörmann et al.

[Title Page](#)[Abstract](#)[Introduction](#)[Conclusions](#)[References](#)[Tables](#)[Figures](#)[⏪](#)[⏩](#)[◀](#)[▶](#)[Back](#)[Close](#)[Full Screen / Esc](#)[Printer-friendly Version](#)[Interactive Discussion](#)

---

**Systematic  
investigation of BrO  
in volcanic plumes  
with GOME-2**C. Hörmann et al.

---

[Title Page](#)[Abstract](#)[Introduction](#)[Conclusions](#)[References](#)[Tables](#)[Figures](#)[⏪](#)[⏩](#)[◀](#)[▶](#)[Back](#)[Close](#)[Full Screen / Esc](#)[Printer-friendly Version](#)[Interactive Discussion](#)

findings widely agreed with the former predictions. The rapid production of BrO inside the downwind plume could thus be explained by directly emitted HBr, which is oxidized in an autocatalytic reaction cycle involving sulphate aerosols and solar radiation as well as the destruction of O<sub>3</sub>. These procedures are associated with the mechanism known as the “bromine explosion”, a reaction cycle that is closely related to the formation of BrO during polar spring and linked to tropospheric ozone depletion events (McConnell et al., 1992; Fan and Jacob, 1992; Platt and Lehrer, 1996; Wennberg, 1999; von Glasow and Crutzen, 2003; Simpson et al., 2007). Other studies by Bobrowski et al. (2007) and Louban et al. (2009) showed both enhanced BrO vertical column densities (VCDs) and BrO/SO<sub>2</sub> ratios toward the edges of the volcanic plume of Mt. Etna, in good agreement to model studies (Bobrowski et al., 2007; von Glasow, 2010), where the increase is caused by the entrainment of O<sub>3</sub>-rich ambient air into the plume devoid of O<sub>3</sub>. Additionally, a case study of day- and nighttime measurements at Masaya volcano (Nicaragua) by Kern et al. (2008), using Long Path Differential Optical Absorption Spectroscopy (LP-DOAS), showed no evidence for BrO during nighttime, while a BrO/SO<sub>2</sub> ratio of up to  $6.4 \times 10^{-5}$  was observed during daytime. This confirmed the suggestion that the reaction cycle is photolytically driven. Furthermore, the long-term development of BrO/SO<sub>2</sub> ratios from ground-based MAX-DOAS measurements at Mt. Etna during 2006–2009 have been recently investigated for its variability in relation to volcanic processes, and it was supposed that the BrO/SO<sub>2</sub> ratio can serve as a parameter to indicate the volcano’s state (Bobrowski and Giuffrida, 2012).

Given the numerous spectroscopic BrO measurements in volcanic plumes and the general ability of satellite instruments to monitor BrO globally (e.g. Wagner and Platt, 1998; Richter et al., 2002; Theys et al., 2011), it appears like an obvious idea to investigate satellite data also for BrO during volcanic events. However, a first attempt to detect volcanic BrO from space, using data from the GOME and the SCIAMACHY (Scanning Imaging Absorption Spectrometer for Atmospheric Chartography) instruments, failed (Afe et al., 2004): no correlation between enhanced columns of SO<sub>2</sub> and the corresponding BrO columns was found in the plumes of selected eruptions at Mt. Etna,





were determined in the same area. Furthermore, in the framework of a SO<sub>2</sub> comparison study between GOME-2 and the DLR Falcon aircraft at Eyjafjallajökull, mean BrO/SO<sub>2</sub> ratios were calculated for some days of the satellite observations in May 2010 that varied from 1.1–2.1 × 10<sup>-4</sup> (Rix et al., 2012).

Motivated by these findings, we analysed the whole dataset of GOME-2 from the beginning of the regular measurements in January 2007 until the end of June 2011 in order to find further volcanic events in the satellite data where BrO might have been detected in the corresponding plumes. For that purpose, volcanic plumes were automatically extracted from the data by identifying clusters of significantly enhanced SO<sub>2</sub> SCDs. Since SO<sub>2</sub> is the third most abundant gaseous species emitted by volcanoes (Textor et al., 2004) and is normally easy to detect in the UV due to its strong differential absorption features, it is well-suited as a proxy for the existence and extent of a volcanic plume. The area covered by each captured SO<sub>2</sub> plume was investigated for a simultaneous enhancement of BrO. Afterwards, the data were checked for the degree of spatial correlation between the two species and the BrO/SO<sub>2</sub> ratios were calculated.

The paper is structured as follows: After a short description of the GOME-2 satellite instrument and the DOAS retrieval for SO<sub>2</sub> and BrO in Sect. 2, the volcanic plume extraction algorithm, the background correction for non-volcanic BrO (respectively SO<sub>2</sub>) and the approach for dealing with saturation effects in the SO<sub>2</sub> retrieval during major volcanic eruptions are introduced in Sect. 3. Section 4 presents the results, showing several examples for different BrO/SO<sub>2</sub> relationships from the identified volcanic plumes. Subsequently, in Sect. 5, all extracted volcanic plumes are systematically analysed and categorized according to their BrO/SO<sub>2</sub> relationship. A discussion of the results in Sect. 6 is followed by final conclusions in Sect. 7.

## 2 Instrument and data retrieval

The GOME-2 (Global Ozone Monitoring Experiment-2) is the first of three identical instruments that are part of the MetOp satellite series operated by the European

### Systematic investigation of BrO in volcanic plumes with GOME-2

C. Hörmann et al.

Title Page

Abstract

Introduction

Conclusions

References

Tables

Figures

⏪

⏩

◀

▶

Back

Close

Full Screen / Esc

Printer-friendly Version

Interactive Discussion



---

**Systematic  
investigation of BrO  
in volcanic plumes  
with GOME-2**C. Hörmann et al.

---

[Title Page](#)[Abstract](#)[Introduction](#)[Conclusions](#)[References](#)[Tables](#)[Figures](#)[⏪](#)[⏩](#)[◀](#)[▶](#)[Back](#)[Close](#)[Full Screen / Esc](#)[Printer-friendly Version](#)[Interactive Discussion](#)

Organisation for the Exploitation of Meteorological Satellites (EUMETSAT). MetOp-A was launched into a sun-synchronous polar orbit at 800 km altitude in October 2006 (Callies et al., 2000) (the second and third GOME-2 instrument will be carried by MetOp-B and MetOp-C in 2012 and 2018, respectively). The satellite crosses the equator at 9:30 local time. GOME-2 is a 4 channel UV/Vis grating spectrometer that observes the Earth's atmosphere in nadir viewing geometry. By scanning the earth surface with a swath-width of 1920 km (including viewing angles up to 50° off-nadir), global coverage is achieved within 1.5 days (EUMETSAT, 2005; Munro et al., 2006). GOME-2 measures both the radiance component of sunlight reflected by the Earth's atmosphere and the direct sunlight, covering the wavelength region of 240–790 nm at moderate spectral resolution of 0.2–0.4 nm. With a pixel size of 40 × 80 km<sup>2</sup>, GOME-2 observes 4 times smaller ground pixels than its predecessor GOME on ERS-2.

## 2.1 Standard DOAS retrieval for SO<sub>2</sub> and BrO

The satellite data were analysed using the Differential Optical Absorption Spectroscopy (DOAS) technique (Platt and Stutz, 2008). For our SO<sub>2</sub> standard retrieval (SO<sub>2</sub> SR), the wavelength range 312.1–324 nm was used. Apart from a cross section for SO<sub>2</sub> (Bogumil et al., 2003, 273 K), an O<sub>3</sub> cross section (Gür et al., 2005, 223 K), the individual Sun Mean Reference Spectrum (SMR) from GOME-2 for each day (containing no atmospheric absorptions), the Ring spectrum (calculated from the SMR – see Wagner et al., 2009) and the inverse SMR spectrum were included into the fitting process (the inverse SMR spectrum is a first-order correction for possible spectrographic stray light). Since the length of atmospheric light paths changes systematically with wavelength (e.g. Van Roozendaal et al., 2006a), not only the original O<sub>3</sub> absorption cross section, but also a second one (the original cross section scaled with a fourth order polynomial in wavelength) was included. A 5th order polynomial was applied to account for the broad-band structures and a small wavelength shift was allowed for the measured spectra.

**Systematic  
investigation of BrO  
in volcanic plumes  
with GOME-2**

C. Hörmann et al.

Title Page

Abstract

Introduction

Conclusions

References

Tables

Figures

◀

▶

◀

▶

Back

Close

Full Screen / Esc

Printer-friendly Version

Interactive Discussion



For the BrO retrieval, the wavelength range from 336–360 nm was used, which contains 4 adjacent absorption bands (Sihler et al., 2012). In addition to the BrO cross section from Wilmouth et al. (1999, 228 K), ozone cross sections at 223 and 243 K (Gür et al., 2005), O<sub>4</sub> (Greenblatt et al., 1997), NO<sub>2</sub> (Vandaele et al., 2002, 220 K), OClO (Bogumil et al., 2003, 293 K) and SO<sub>2</sub> (Bogumil et al., 2003, 273 K) were included in the retrieval. As in the case of the SO<sub>2</sub> fit, the SMR, a Ring spectrum, an inverse spectrum (calculated from the SMR) and a 5th order polynomial were also included in the BrO retrieval.

## 2.2 Alternative SO<sub>2</sub> retrieval in the case of very high SO<sub>2</sub> SCDs

During phases of explosive eruptions, very high SO<sub>2</sub> SCDs ( $> 1 \times 10^{18}$  molecule cm<sup>-2</sup>) can be observed in some parts of the detected volcanic plumes. In such cases, the absorption in the standard SO<sub>2</sub> wavelength fit range (in this study 312.1–324 nm) can become so strong, that only the outermost layers of the volcanic plume are actually penetrated by the incident sunlight, and no light from inner parts of the plume or below is detected within the analysed wavelength range (Bobrowski et al., 2010). Consequently, the measurement will not be sensitive to the entire plume, i.e. the effective airmass factor (AMF) will be largely reduced for parts of the plume, leading to an underestimation of the “true” SO<sub>2</sub> SCDs in the SO<sub>2</sub> standard retrieval (see Sect. 2.1).

Previous attempts to correct for this non-linearity due to saturation effects relied on iterative model approaches (e.g. Yang et al., 2007, 2009; Richter et al., 2009), but such approaches are rather time consuming and need much computing power. Also, usually insufficient knowledge on aerosol and cloud properties is available, which also affect the measured spectra. Therefore, we decided to switch to an alternative evaluation fit range at slightly longer wavelength (326.5–335.3 nm), where the SO<sub>2</sub> absorption is weaker and thus the response of the resulting SO<sub>2</sub> SCDs is linear even at high SO<sub>2</sub> concentrations. In the following we refer to this alternative retrieval as the “SO<sub>2</sub> AR”. For the SO<sub>2</sub> AR, again the O<sub>3</sub> cross sections from Gür et al. (2005, 223 K and 243 K) were used, as well as those for SO<sub>2</sub> (Bogumil et al., 2003, 273 K), the SMR, a Ring

**Systematic investigation of BrO in volcanic plumes with GOME-2**

C. Hörmann et al.

Title Page

Abstract

Introduction

Conclusions

References

Tables

Figures

⏪

⏩

◀

▶

Back

Close

Full Screen / Esc

Printer-friendly Version

Interactive Discussion



spectrum, an inverse spectrum (calculated from the SMR) and a 5th order polynomial. Although the sensitivity in the alternative wavelength range is clearly reduced in comparison to the standard fit range (the differential absorption cross section of SO<sub>2</sub> is about 2–3 magnitudes lower than for the SO<sub>2</sub> SR), this disadvantage is mostly compensated by the increased intensity of light towards longer wavelengths ( $\lambda$ ) due to weaker absorption, less Rayleigh scattering (proportional to  $\lambda^{-4}$ ) and thus higher AMFs. The evaluation at longer wavelengths in the case of large SO<sub>2</sub> SCDs therefore has the advantage that the signal-to-noise ratio is clearly increased, while the observed radiation has typically penetrated the whole plume. In Fig. 1, an example for both SO<sub>2</sub> DOAS retrievals (as well as for the BrO fit) is given for the volcanic plume of the Kasatochi eruption on 9 August 2008 (see also Fig. 10). While the SO<sub>2</sub> absorption features can be generally detected for the SO<sub>2</sub> SR, the residual shows significant systematic structures that are caused by the non-linearity of the DOAS fit in cases of very strong SO<sub>2</sub> absorption (Fig. 1a). The resulting SO<sub>2</sub> SCD is  $(4.6 \pm 0.3) \times 10^{18}$  molecule cm<sup>-2</sup> with a residual RMS of  $4.8 \times 10^{-2}$ . The fit results of the same GOME-2 pixel for the SO<sub>2</sub> AR in Fig. 1b clearly shows reduced systematic residual structures and a resulting SO<sub>2</sub> SCD of  $(1.9 \pm 0.1) \times 10^{19}$  molecule cm<sup>-2</sup>, which is about 4 times higher than for the SO<sub>2</sub> SR. Additionally, the RMS of the residual is now about 40 times lower ( $1.2 \times 10^{-3}$ ) compared to the SO<sub>2</sub> SR. The BrO fit and residual of the BrO DOAS retrieval are additionally shown in Fig. 1c and indicate the presence of enhanced BrO SCDs in the volcanic plume. In order to use the advantages of the different evaluation schemes (high sensitivity of the SO<sub>2</sub> SR for small SCDs and no saturation of the SO<sub>2</sub> AR for high SCDs), we merged the SO<sub>2</sub> SR and the SO<sub>2</sub> AR to one “combined” SO<sub>2</sub> product. A detailed description how the results from both retrievals are merged for this combined SO<sub>2</sub> product will be given in Sect. 3.5.

### 3 Systematic study of volcanic BrO using GOME-2

The GOME-2 dataset was investigated for the simultaneous observation of volcanic SO<sub>2</sub> and BrO since the start of the regular measurements in January 2007 until the end of June 2011. Since SO<sub>2</sub> is the third most abundant gaseous species that is emitted by a volcano after H<sub>2</sub>O and CO<sub>2</sub> (Textor et al., 2004), it has been used as a tracer in order to identify volcanic plumes in the satellite data. In total, 553 days with significantly enhanced SO<sub>2</sub> SCDs were found in the dataset, which were due to increased activity or eruptive phases of at least 37 volcanoes worldwide (the spatial proximity of several active volcanoes in some regions, e.g. the Kamchatka Peninsula, and the lack of local observations lead to the problem that the plume could not be unequivocally assigned to one specific volcano in some cases). Since enhancements of BrO columns in this study are only investigated for enhanced SO<sub>2</sub> columns, no statement can be made about the (very unlikely) case, where SO<sub>2</sub> is below the detection limit, while enhanced BrO SCDs could be observed in a volcanic plume.

#### 3.1 Automatic capturing of volcanic SO<sub>2</sub> plumes

In order to detect SO<sub>2</sub> plumes that are associated with increased activity or eruptive phases of volcanoes, the GOME-2 data was analysed using a newly developed detection algorithm that searches the dataset for conspicuously elevated SO<sub>2</sub> columns. Similar approaches have been developed during the last years in the course of operational early-warning systems for volcanic ash (e.g. Richter, 2009; SACS, 2012). Such early-warning systems provide rapid information to the aviation community about the location of a volcanic plume, which might compromise the safety of airplanes if they contain ash. Whereas these projects focus on near-real time early-warnings for volcanic ash plumes, the focus of our algorithm lies on the offline identification of volcanic plumes and especially the accurate extraction of SO<sub>2</sub>-affected satellite pixels in order to compare the associated SO<sub>2</sub> SCDs with those of BrO in the GOME-2 dataset. Not only the reliable identification of volcanic plumes in the satellite data is needed, but

### Systematic investigation of BrO in volcanic plumes with GOME-2

C. Hörmann et al.

Title Page

Abstract

Introduction

Conclusions

References

Tables

Figures

⏪

⏩

◀

▶

Back

Close

Full Screen / Esc

Printer-friendly Version

Interactive Discussion



also a more sophisticated correction for the non-volcanic BrO background signal in the vicinity of volcanic plumes.

### 3.2 Global maps with two days coverage

In a first step, the so-called “geometrical” SO<sub>2</sub> VCDs for all GOME-2 pixels were calculated from the SCDs by the use of geometrical airmass factors (AMFs):

$$\text{VCD}_{i,\text{geo}} = \frac{\text{SCD}_i}{\text{AMF}_{i,\text{geo}}} \quad (1)$$

$$\text{AMF}_{i,\text{geo}} = \frac{1}{\cos(\theta_i)} + \frac{1}{\cos(\xi_i)} \quad (2)$$

where  $\theta_i$  is the line of sight (LOS; nadir = 0°) and  $\xi_i$  is the solar zenith angle (SZA) during the measurement of satellite pixel  $i$ .

In the following, the data for two consecutive days were projected on gridded global maps covering two days at a grid resolution of 0.5° × 0.5°. These two days global maps (TDGM) differ from the commonly used layout for operational GOME-2 DOAS products, where all measurements of satellite orbits that had started within the regarded day (start time 00:00:00–23:59:59 UTC) are projected on a single global map (−90° N to +90° N and −180° E to +180° E). By using the TDGMs, we overcome a serious disadvantage of single day maps that is due to the occurrence of a temporal discontinuity in the illustration of data from satellites operating in sun-synchronous orbits. Figure 2a shows the GOME-2 satellite orbits for two consecutive days next to each other (day 1 on the right, day 2 on the left side). As the first and the last orbit of a single day is typically located at more than +105° E and extends up to +180° E and beyond, adjacent and/or overlapping pixels exhibit a time shift of up to 24 h (area between the light blue and green satellite orbits during day 1 and the green and dark red orbits during day 2 in Fig. 2a). Additionally, the orbits overlap at high latitudes (respectively low latitudes during arctic winter), so that also here time shifts of up to 10 h may occur between individual neighbouring satellite pixels. For the analysis of volcanic plumes

## Systematic investigation of BrO in volcanic plumes with GOME-2

C. Hörmann et al.

Title Page

Abstract

Introduction

Conclusions

References

Tables

Figures

⏪

⏩

◀

▶

Back

Close

Full Screen / Esc

Printer-friendly Version

Interactive Discussion





that might be located at the edge of single day maps, the associated data can not be illustrated properly by simply sticking the maps of two consecutive days together, as another time shift of  $\sim 24$  h occurs at the intersecting region between day 1 and day 2. Therefore, the data in the TDGM was gridded in such a way that the chronology of the satellite orbits in direct succession is conserved in western direction (Fig. 2b). As the data has also been restricted to latitudes from  $-70^\circ$  N to  $+70^\circ$  N and  $SZA < 70^\circ$  for this study, most overlapping pixels at high latitudes are skipped. Remaining overlapping pixels with a measurement time difference of more than  $\sim 3.5$  h (13 000 s) were discarded. By using the chronologically correct projection on the TDGM (that now extends from  $-540^\circ$  E to  $+180^\circ$  E in longitudinal direction), the temporal discontinuity can be avoided. The thus filtered satellite data within  $-180^\circ$  E to  $+180^\circ$  E now consequently contain all  $SO_2$  fit results that were observed during the first regarded day (parts of the first 2 orbits at the eastern boundary of day 1 usually belong to the previous day), while most of the data within  $-540^\circ$  E to  $-180^\circ$  E contains the  $SO_2$  columns for the following day. The most important advantages of the TDGMs are (1) being able to identify volcanic plumes close to the first or the last orbit of satellites in sun-synchronous orbits and (2) the ability to capture the complete plume, even if it extends beyond the common map boundaries in westerly direction ( $< -180^\circ$  E).

In order to prevent the detection of  $SO_2$  events that are caused by non-volcanic emissions and/or measurement errors, the data for several areas are masked out. These include in particular the greater area of Eastern China, Norilsk (Russia) and the Highveld plateau (South Africa), where anthropogenic  $SO_2$  emissions can be regularly detected (caused e.g. by huge industrial coal plant and/or heavy metal smelter complexes), but also large parts of South America, where the satellite measurements are strongly influenced by the South Atlantic Anomaly (SAA) of the radiation belt. The excluded areas can be found in Table 1.

---

**Systematic investigation of BrO in volcanic plumes with GOME-2**C. Hörmann et al.

---

[Title Page](#)[Abstract](#)[Introduction](#)[Conclusions](#)[References](#)[Tables](#)[Figures](#)[⏪](#)[⏩](#)[◀](#)[▶](#)[Back](#)[Close](#)[Full Screen / Esc](#)[Printer-friendly Version](#)[Interactive Discussion](#)

### 3.3 Volcanic plume extraction

After the data were projected on the TDGM, the SO<sub>2</sub> VCDs were corrected for an offset (usually caused by interferences with the O<sub>3</sub> absorption cross section and/or imperfect fitting of the Ring effect). For this purpose, the median in longitudinal direction for each grid pixel row (0.5°) was subtracted from the data. The offset corrected data were then subdivided into boxes of 5° × 5° (10 × 10 grid pixels, for an example see Fig. 3). All boxes were investigated for a maximum SO<sub>2</sub> VCD of at least 5 × 10<sup>16</sup> molecule cm<sup>-2</sup>, indicating that a box might contain a volcanic plume. This threshold was found to be well above the detection limit of the instrument and is consistent with typical SO<sub>2</sub> VCDs that are measured during strong degassing episodes and minor volcanic eruptions. Please note that, according to our data, the SO<sub>2</sub> detection limit has increased from approximately 1 × 10<sup>16</sup> molecule cm<sup>-2</sup> in 2007 to more than 2 × 10<sup>16</sup> molecule cm<sup>-2</sup> in June 2011 due to instrument degradation (for a detailed analysis of the impacts of the GOME-2 degradation on Level 2 products see also Dikty and Richter, 2011). However, since single erroneous measurements might sometimes also cause SO<sub>2</sub> VCD of comparable magnitude, all direct neighbouring grid pixels were additionally investigated using a second, lower SO<sub>2</sub> VCD threshold of 3 × 10<sup>16</sup> molecule cm<sup>-2</sup>, to ensure the actual presence of an enhanced SO<sub>2</sub> VCD cluster inside the box area. Whenever at least 4 neighbouring grid pixels exceeded the second threshold, the box was assumed to contain at least parts of a volcanic SO<sub>2</sub> plume (see dark red boxes in Fig. 3). For each identified “SO<sub>2</sub> plume event box” (in the following abbreviated as “SO<sub>2</sub> PEB”), all directly neighbouring boxes were also assigned to this specific event in order to prevent losing parts of the volcanic plume where the VCDs were not sufficiently high to be identified as an independent SO<sub>2</sub> PEB (yellow boxes in Fig. 3). After all plume affected boxes had been determined, resulting clusters of SO<sub>2</sub> PEBs (red and yellow boxes) represent individual SO<sub>2</sub> plumes for the regarded days. In order to obtain a reference area next to the captured SO<sub>2</sub> plume events, all non-SO<sub>2</sub> PEBs within another surrounding box

(that extends from  $\pm 5^\circ$  from the maximum/minimum latitudinal/longitudinal grid pixel position of the SO<sub>2</sub> PEB cluster) were registered (green boxes in Fig. 3).

To prevent the algorithm from capturing the same plume twice (as it always considers the data of two consecutive days), only SO<sub>2</sub> events that consist completely of satellite pixels recorded during the first regarded day or on the first and the following day were accepted for further investigation. Therefore, a SO<sub>2</sub> event that consists exclusively of measurements from the second of the two regarded days during an iteration of the algorithm was not captured until the subsequent iteration. This also means that the detection of a possible (but highly unlikely) case of a volcanic plume that encompasses the whole globe cannot be captured in its full extent using this approach. To the authors' knowledge, such an event has not occurred since the launch of GOME-2.

### 3.4 Non-volcanic background correction and plume pixel selection

Gridded satellite data are much easier to handle by the plume detection algorithm (see Sect. 3.3), because of the grid's regular geometry. Additionally, it has the advantage that background noise partly averages out during the gridding process, so that the misidentification of satellite measurements outside of a volcanic plume is prevented. However, for the further analysis of the volcanic plume events, the original GOME-2 ground-pixels associated with the registered grid boxes were regarded, as they represent the actual satellite measurements. In particular individual satellite pixels have to be used for the correlation analysis between SO<sub>2</sub> and BrO, because the spatial patterns of both species are generally different.

For the detailed analysis of the BrO columns inside the detected volcanic SO<sub>2</sub> plumes and a possible correlation of the two species, the SCDs for SO<sub>2</sub> and BrO from the GOME-2 measurements need to be corrected for a non-volcanic offset. In contrast to the previous background correction process for the gridded satellite data, the lat-/longitudinal offset was now corrected in a more sophisticated way. While the offset of SO<sub>2</sub> is mainly caused by the spectral interference with stratospheric ozone and/or the imperfect fitting of the Ring effect (see also Heue et al., 2011), the volcanic BrO signal

## Systematic investigation of BrO in volcanic plumes with GOME-2

C. Hörmann et al.

Title Page

Abstract

Introduction

Conclusions

References

Tables

Figures



Back

Close

Full Screen / Esc

Printer-friendly Version

Interactive Discussion



is superimposed by the stratospheric BrO distribution, which systematically depends on latitude, but to a smaller degree also on longitude. Additionally, extended areas in high latitudes might be affected by tropospheric BrO plumes that are formed e.g. at the sea ice surface during Arctic spring in polar regions and can sometimes extend to latitudes of  $\pm 70^\circ$  N (Wagner and Platt, 1998). In a first step, the geometric AMF was used to convert SCDs to VCDs for both species (see also Sect. 3.3). This is a reasonable approach, as we are here mainly interested in correcting the influence of stratospheric BrO and  $\text{O}_3$  to the resulting SCDs for BrO and  $\text{SO}_2$  respectively. For the determination of the latitudinal/longitudinal dependent offset of  $\text{SO}_2$ , a 2-dimensional spatial polynomial fit of 3rd degree was applied to the pixels from the reference area of the  $\text{SO}_2$  PEB cluster (Fig. 3) and those pixels from the PEB cluster itself, whose  $\text{SO}_2$  VCDs lay within  $3\sigma$  of the reference area (and were therefore supposed to be located outside the volcanic plume):

$$\text{SO}_2 \text{VCD}_{i,\text{offset}} \approx \sum_{m,n=0}^3 a_{mn} \times x_i^m \times y_i^n \quad (3)$$

where  $a_{mn}$  are the fitted  $\text{SO}_2$  offset VCDs at the centre coordinates  $x$  and  $y$  [ $^\circ$ ] of the satellite pixel  $i$ . All other satellite pixels within the PEB cluster ( $\text{SO}_2$  VCD  $> 3\sigma$  of the combined reference area) were now, in a first step, assumed to be part of the volcanic plume. Similarly, the corresponding BrO VCD $_{i,\text{geo}}$  were approximated by a 2-dimensional polynomial of 4th degree ( $m, n = 0, \dots, 4$ ). The higher degree of the polynomial compared to the  $\text{SO}_2$  background approximation was chosen because of the generally stronger spatial gradients of the BrO VCDs. By subtracting the fitted polynomials from all VCDs (including the VCDs from the presumed volcanic plume pixels), we obtained the offset corrected geometrical vertical column densities VCD $_i^*$ :

$$\text{VCD}_i^* = \text{VCD}_{i,\text{geo}} - \text{VCD}_{i,\text{offset}} \quad (4)$$

**Systematic investigation of BrO in volcanic plumes with GOME-2**

C. Hörmann et al.

Title Page

Abstract

Introduction

Conclusions

References

Tables

Figures

⏪

⏩

◀

▶

Back

Close

Full Screen / Esc

Printer-friendly Version

Interactive Discussion



All offset/background corrected pixels within the SO<sub>2</sub> PEB cluster were then once again checked for pixels whose VCD<sub>*i*</sub><sup>\*</sup> exceeded 3σ of the offset-corrected combined reference area. These pixels finally represented the identified volcanic plume.

Despite the different evaluation wavelength ranges, the AMF of the two species should only depend slightly on the altitude of the volcanic plume during most detected SO<sub>2</sub> events, with typical plume heights between 7 and 13 km (see Afe et al., 2004). However, the presence of volcanic ash might have an important influence on radiative transfer and therefore further information (e.g. about plume height and ash content) is necessary for a precise VCD calculation. As the focus of this study lies in the general ability of the GOME-2 instrument to detect BrO in addition to SO<sub>2</sub> during increased activity/eruptive phases of volcanoes (and the possible correlation between them), we simply reconverted the background corrected VCD<sub>*i*</sub><sup>\*</sup> into slant column densities SCD<sub>*i*</sub><sup>\*</sup> for the following investigations by multiplication with their AMF<sub>*i,geo.*</sub>:

$$SCD_i^* = VCD_{i,geo.}^* \times AMF_{i,geo.} \quad (5)$$

### 3.5 Combination of SO<sub>2</sub> standard and alternative retrieval for major eruptions

Particularly for major volcanic events, we have to account for non-linearities in the SO<sub>2</sub> retrieval, while for minor events, the standard retrieval is more appropriate. Thus, for the automatic plume extraction algorithm, both retrievals had to be combined. For all detected volcanic plumes where the maximum SO<sub>2</sub> SCD exceeded 1 × 10<sup>18</sup> molecule cm<sup>-2</sup>, the results from the SO<sub>2</sub> AR were investigated for the same PEB clusters and associated reference areas as for the standard retrieval. The geometrical SO<sub>2</sub> VCDs from the AR were offset corrected in the same way as the VCDs from the SR (see Sect. 3.4). Again, all satellite pixels within the PEB cluster with a SO<sub>2</sub> VCD > 3σ of the offset corrected reference area were assumed to be part of the volcanic plume. Maps of the SO<sub>2</sub> plume were finally created by using the initial plume pixels from the SR, but all pixels with a SO<sub>2</sub> SCD > 1 × 10<sup>18</sup> molecule cm<sup>-2</sup> were replaced by the results from the AR, if the corresponding pixels were also found to be

## Systematic investigation of BrO in volcanic plumes with GOME-2

C. Hörmann et al.

Title Page

Abstract

Introduction

Conclusions

References

Tables

Figures

⏪

⏩

◀

▶

Back

Close

Full Screen / Esc

Printer-friendly Version

Interactive Discussion



## Systematic investigation of BrO in volcanic plumes with GOME-2

C. Hörmann et al.

Title Page

Abstract

Introduction

Conclusions

References

Tables

Figures

⏪

⏩

◀

▶

Back

Close

Full Screen / Esc

Printer-friendly Version

Interactive Discussion



part of the plume after the background correction process. In Fig. 4, the SO<sub>2</sub> plume from the Kasatochi eruption is shown for the 9 August 2008 (please note the logarithmic scale in Fig. 4a, b, d). While the maximum SO<sub>2</sub> SCD for the SR (Fig. 4a) is located in the south-eastern part of plume (indicated by the small black star), it is shifted towards west for the AR (Fig. 4b). Additionally, the resulting SO<sub>2</sub> SCDs for the AR are now up to 5 times higher than for the SR, as can be seen in Fig. 4c, where the ratios of the resulting SO<sub>2</sub> columns from the different retrievals are shown for all pixels that were identified to be part of the plume in both evaluation wavelength regions. Results from both retrievals are finally combined in Fig. 4d. The plume's centre now looks much more structured than for the SR, where the central part of the plume mainly consists of a large homogeneous area, as most of the SO<sub>2</sub> SCDs seem to be scattered around  $5 \times 10^{18}$  molecule cm<sup>-2</sup> due to the saturation effect.

## 4 Results

The analysis of the GOME-2 measurements during the time period between January 2007 and June 2011 resulted in 772 SO<sub>2</sub> PEB clusters on 553 days, representing individual or at least completely isolated parts of volcanic plumes. Therefore 33.7 % of all considered days (1642 days in total) showed signs of enhanced volcanic activity and/or eruptions in the satellite data. However, by looking at all captured events in the investigated satellite data, it becomes clear, that a general problem remains in identifying the source of some volcanic plumes in areas where several highly active volcanoes are located in close proximity. This is especially the case for the volcanoes on Kamchatka which houses about 29 active volcanoes. Whenever the origin of a volcanic plume could not clearly be identified, the most likely volcano is named. For that purpose, we cross-checked our data with online reports on the Global Volcanism Program (GVP) website of the Smithsonian Institution (available under <http://www.volcano.si.edu/reports/usgs/>) and additionally with daily SO<sub>2</sub> maps from the Ozone Monitoring Instrument (OMI, <http://so2.gsfc.nasa.gov/>), the latter providing a more detailed spatial resolution of up

to  $13 \times 25 \text{ km}^2$  (compared to  $40 \times 80 \text{ km}^2$  for GOME-2) and also daily global coverage. In Fig. 5, time series of the maximum VCDs\* from our GOME-2 evaluation for  $\text{SO}_2$  and BrO within all identified volcanic plumes are shown. Apart from many moderate eruptions and strong degassing volcanic events, several major eruptions are clearly visible in the time series, e.g. the eruptions of Okmok (Aleutian Islands, July 2008), Kasatochi (Aleutian Islands, August 2008), Sarychev (Kuril Islands, June 2009), Merapi (Indonesia, November 2010), Grímsvötn (Iceland, April 2011) and Nabro (Eritrea, June 2011). For the BrO VCDs\*, the time series indicates the presence of volcanic BrO during some of the monitored  $\text{SO}_2$  events. While the maximum BrO VCD\* for most of the volcanic events is around  $2.5 \times 10^{13} \text{ molecule cm}^{-2}$ , the VCDs\* during several eruptions show much higher values.

In the following, several volcanic eruptions will be presented and discussed in more detail in order to investigate the different  $\text{SO}_2$  to BrO relationships that have been observed. For this purpose, we will focus on some of those volcanic plumes where the BrO VCD\*<sub>max</sub> exceeded  $5 \times 10^{13} \text{ molecule cm}^{-2}$  and therefore indicate the presence of volcanic BrO. This includes the eruptions of BZ – Bezymianny (Kamchatka Peninsula) in May 2007, ET – Mt. Etna in May 2008, KS – Kasatochi volcano in August 2008, DL – Dalaffilla (Ethiopia) in November 2008, RD – Mt. Redoubt (Alaska) in March/April 2009, SA – Sarychev (Kuril Islands) in June 2009, EY – Eyjafjallajökull (Iceland) in April/May 2010 and NB – Nabro volcano in June 2011 (see labelled time periods in Fig. 5 and Table 2, respectively). The sequence of selected examples starts with volcanic plumes which show a high correlation and continues with examples of decreasing degree of correlation. All examples are examined for linear correlation between the two species by applying a bivariate linear fit (Cantrell, 2008) to the  $\text{SO}_2$  and BrO SCDs\* of the identified plume pixels.

**Systematic investigation of BrO in volcanic plumes with GOME-2**

C. Hörmann et al.

Title Page

Abstract

Introduction

Conclusions

References

Tables

Figures

⏪

⏩

◀

▶

Back

Close

Full Screen / Esc

Printer-friendly Version

Interactive Discussion





## 4.1 Etna (14 May 2008) – ET

Being one of the most active volcanoes in the world and easily accessible, Etna is one of the most frequently monitored volcanoes. According to reports from the Istituto Nazionale di Geofisica e Vulcanologia, sezione di Catania (INGV-CT), a new eruptive fissure opened on Etna's upper east side on 13 May, after several months of seismic unrest (Smithsonian, 2007–2011). Figure 6 shows the volcanic plume during the eruption on 14 May 2008 (labelled ET in Fig. 5). The SO<sub>2</sub> and BrO SCDs\* of the whole regarded area (including the plume and reference area) can be seen in Fig. 6a, c, respectively. Figure 6b, d show only the satellite pixels where the SO<sub>2</sub> VCDs\* were larger than 3σ\* (with σ\* the standard deviation of the reference area). The corresponding correlation plot (Fig. 6e) shows a clear linear correlation between the two species with  $r^2 = 0.7$  and a fitted mean BrO/SO<sub>2</sub> ratio of  $\sim 2.5 \times 10^{-4}$ . It is interesting to mention, that the location of the SO<sub>2</sub> SCD\*<sub>max</sub> corresponds to the location of the BrO SCD\*<sub>max</sub>. Another eruption at the Southeast Crater of Mt. Etna on 10 May 2008 (Bonaccorso et al., 2011) showed similar behaviour, with a linear correlation between the two species and BrO/SO<sub>2</sub> ratios of some 10<sup>-4</sup>.

## 4.2 Bezymianny/Kliuchevskoi (11/12 May 2007) – BZ

The Bezymianny volcano is one of 29 active volcanoes on the Kamchatka Peninsula. The volcano was moderately active throughout the whole year 2007, interrupted by some small explosions in May and October–December. Figure 7 shows the trace gas distribution after such an explosion of the volcano on 11/12 May 2007 (labelled BZ in Fig. 5). In Fig. 7a, the background corrected volcanic SO<sub>2</sub> plume after the explosion of Bezymianny (indicated by the orange triangle) can be seen over the Kamchatka Peninsula. Below (Fig. 7c), the BrO SCDs\* are shown for the same area, indicating the presence of enhanced BrO columns in the same area as the enhanced SO<sub>2</sub> SCDs\*. Like for the previous example of Mt. Etna, Fig. 7b, d show only the satellite pixels that were assumed to contain the volcanic plume (SO<sub>2</sub> VCDs\* > 3σ\*). These pixels

### Systematic investigation of BrO in volcanic plumes with GOME-2

C. Hörmann et al.

Title Page

Abstract

Introduction

Conclusions

References

Tables

Figures

⏪

⏩

◀

▶

Back

Close

Full Screen / Esc

Printer-friendly Version

Interactive Discussion



were used for the correlation plot (Fig. 7e), with a correlation coefficient  $r^2 = 0.62$  and a resulting mean BrO/SO<sub>2</sub> ratio of  $\sim 4.4 \times 10^{-4}$ .

Due to the close spatial proximity of Bezymianny to the Kliuchevskoi volcano ( $\sim 10$  km), we can not be entirely sure that the observed volcanic plume came from Bezymianny alone, as Kliuchevskoi showed also increased activity at the time of the measurements according to reports of the Kamchatka Volcanic Eruption Response Team (KVERT). However, as seismic data suggested an explosive eruption of Bezymianny shortly before the satellite measurements (Smithsonian, 2007–2011), it seems most likely that the major part of the visible plume originated from Bezymianny with minor parts from Kliuchevskoi (see also the KVERT webpage for detailed activity reports on <http://www.kscnet.ru/ivs/kvert/updates/>).

### 4.3 Dalaffilla (4 November 2008) – DL

On 3 November 2008, an eruption of the Dalaffilla volcano in Ethiopia's Afar region produced an extensive plume of SO<sub>2</sub>, which was rapidly transported in north-eastern direction towards the Arabian Peninsula and reached the western part of China after two days. While the GOME-2 instrument was able to track the SO<sub>2</sub> plume for about 10 days, BrO was only clearly detected on the very first day after the eruption on 4 November, when the plume was also seen for the first time by the satellite instrument (labelled DL in Fig. 5). Figure 8a shows that the SO<sub>2</sub> plume can be separated into two main parts, one with rather high SO<sub>2</sub> SCDs\* over the south-eastern side of the Arabian Peninsula, the other one with lower SO<sub>2</sub> SCDs\* further in the north west. In contrast to these findings, the BrO SCDs\* (Fig. 8c) were only significantly enhanced in the north-western part of the extracted SO<sub>2</sub> plume (Fig. 8b) and in a long band towards the Persian Gulf. The consideration of all identified SO<sub>2</sub> plume pixels therefore leads to no clear linear correlation between the two species, but already indicates that such a correlation might be present in some parts of the plume. If we limit the focus to the plume pixels around the region with the enhanced BrO SCDs\* (indicated by the red

## Systematic investigation of BrO in volcanic plumes with GOME-2

C. Hörmann et al.

Title Page

Abstract

Introduction

Conclusions

References

Tables

Figures

⏪

⏩

◀

▶

Back

Close

Full Screen / Esc

Printer-friendly Version

Interactive Discussion

5 polygon in Fig. 8b, d), a linear correlation between the SO<sub>2</sub> and BrO SCDs\* is found, with  $r^2 = 0.54$  and a mean fitted BrO/SO<sub>2</sub> ratio of  $\sim 6.3 \times 10^{-5}$ . It seems remarkable that no enhanced BrO SCDs\* can be found in the south-eastern part of the plume, while the maximum SCDs\* of SO<sub>2</sub> were observed within this area. Possible reasons for this non-uniform distribution of the enhanced BrO SCDs\* will be discussed in Sect. 6.

#### 4.4 Nabro (16 June 2011) – NB

10 Announced by an earthquake swarm on 12 June 2011, the first recorded eruption of the Nabro volcano (Eritrea, Africa) started one day later in the early morning of 13 June (labelled NB in Fig. 5). As the Afar Triangle area in Southern Eritrea is barely populated, first observations of the eruption by eye witnesses did not occur until the late evening (Smithsonian, 2007–2011), while several satellite instruments (namely GOME-2, SCIAMACHY, OMI, the Atmospheric Infrared Sounder – AIRS – and the Infrared Atmospheric Sounding Interferometer – IASI) were already able to monitor the plume's propagation towards Northern Egypt for about 2000 km during the whole day (SACS, 2012). On the 16 June, the GOME-2 SO<sub>2</sub> measurements (Fig. 9a) show that while the plume front had been transported to Western China the volcano continued to emit significant amounts of SO<sub>2</sub>. From the BrO retrieval (Fig. 9c), enhanced SCDs\* can only be seen clearly within the area of the highest SO<sub>2</sub> SCDs\* that occur about 600–700 km from the volcano. Whenever the volcanic plume was captured by the GOME-2 measurements in the course of the eruption, similar behaviour was found for all days with significantly enhanced SO<sub>2</sub> SCDs\* in June. Taking all SO<sub>2</sub> plume pixels into account (Fig. 9b, d) yields a poor correlation coefficient ( $r^2 = 0.29$ ) of the linear fit, which results mainly from the majority of pixels where the SO<sub>2</sub> SCDs\* were significantly enhanced while the BrO SCD\* were not, causing a strong scattering around zero at low SO<sub>2</sub> slant column densities (Fig. 9e – blue crosses). By restricting the data to the area with clearly enhanced BrO SCDs (indicated by the red shape in Fig. 9b, d), the  $r^2$  value increases to 0.5 (Fig. 9e – red crosses). The rather low fitted mean BrO/SO<sub>2</sub> ratio of

## Systematic investigation of BrO in volcanic plumes with GOME-2

C. Hörmann et al.

Title Page

Abstract

Introduction

Conclusions

References

Tables

Figures

⏪

⏩

◀

▶

Back

Close

Full Screen / Esc

Printer-friendly Version

Interactive Discussion

$1.8 \times 10^{-5}$  suggests that the main reason for the apparent absence of BrO in the aged plume might be that the BrO SCDs no longer exceeded the instruments' detection limit. In addition, the conversion of BrO into other bromine species might also play a role.

#### 4.5 Kasatochi (9 and 11 August 2008) – KS

After an increase in the seismic activity during the first days of August 2008, at least five distinct explosions occurred at the Kasatochi volcano in the afternoon of the 7 August. While the first two explosions produced large ash-poor gas-charged plumes, the third one was relatively ash-rich and emitted massive amounts of SO<sub>2</sub>, which reached the lower stratosphere at about 18 km. The two remaining explosions were of minor intensity and only detected by seismic stations (Neal et al., 2011).

The SO<sub>2</sub> plume was detected the first time on 8 August by several satellite instruments (including GOME-2, SCIAMACHY and OMI) and further tracked for at least one month while the plume circled the globe (labelled KS in Fig. 5). The observation of an extensive BrO cloud in the vicinity of the SO<sub>2</sub> plume by GOME-2 was reported by Theys et al. (2009). In contrast to the SO<sub>2</sub> plume, the BrO could only be clearly tracked for about one week. Yet, the GOME-2 observations of the Kasatochi plume provide so far the longest continuous measurements of a single volcanic BrO plume since the first ground-based measurements of volcanic BrO (Bobrowski et al., 2003). The absolute BrO VCDs\* during the first days of the eruption ( $\sim 2 \times 10^{14}$  molecule cm<sup>-2</sup>) were about a factor of 2–3 larger than for the cases discussed in Sects. 4.1–4.4. While all previously presented eruptions of Mt. Etna, Bezymianny, Dalaffilla and Nabro showed similar spatial distributions for BrO and SO<sub>2</sub> and a linear correlation (at least in parts of the plume), the eruption of Kasatochi showed only a roughly similar spatial pattern between the two observed species, with growing differences in the distribution of the two species while the initial plume was transported towards east. Figure 10 shows the volcanic plume on the second day of the GOME-2 observations (9 August 2008). While the enhanced BrO SCDs\* (Fig. 10c, d) are located in the same area as the captured

### Systematic investigation of BrO in volcanic plumes with GOME-2

C. Hörmann et al.

Title Page

Abstract

Introduction

Conclusions

References

Tables

Figures

⏪

⏩

◀

▶

Back

Close

Full Screen / Esc

Printer-friendly Version

Interactive Discussion

SO<sub>2</sub> plume pixels (Fig. 10a, b), the spatial distribution for BrO appears more circular in shape than the SO<sub>2</sub>. The location of the maximum SCDs\* also differs for both species. The maximum SO<sub>2</sub> SCDs\* are located in the southern region of the plume, while the maximum BrO SCDs\* can be found in the western and eastern part. The correlation plot (Fig. 10e) shows a positive correlation between the species ( $r^2 = 0.24$ ), but also a large scatter in the BrO SCDs\* with increasing SO<sub>2</sub> SCDs\*.

In Fig. 11, the plume is shown 2 days later on 11 August 2008. Whereas the main plume has moved towards the Canadian west coast, several branches reach out from the plume centre in south-western and north-eastern direction (Fig. 11a). The clearly enhanced BrO SCDs\* are located around the centre region of the SO<sub>2</sub> plume, but the distribution of the trace gases within this area is different (Fig. 11c). The map of the extracted plume pixels for BrO (Fig. 11d) in comparison to those for SO<sub>2</sub> (Fig. 11b) indicates that most of the BrO seems to be twisted around the plume centre containing the highest SO<sub>2</sub> SCDs\*. Especially the BrO SCDs\* at the location of the highest SO<sub>2</sub> SCDs\* are not as high as for the surrounding area. This can also be seen in the correlation plot (Fig. 11e), where the BrO SCDs\* are linearly correlated up to SO<sub>2</sub> SCDs\*  $< 5 \times 10^{18}$ . For higher SO<sub>2</sub> SCDs\*, the BrO columns appear to level out around  $2.5 \times 10^{14}$  molecule cm<sup>-2</sup>. One possible reason for such a behaviour might be that the plume centre was not yet entirely mixed with ambient ozone-rich air after sunrise at the time of the GOME-2 measurements.

#### 4.6 Sarychev (15/16 June 2009) – SR

The eruption of the Sarychev volcano (Kuril Islands, Russia) in June 2009 is another example of a complex BrO/SO<sub>2</sub> relationship as seen in the case of Kasatochi (labelled SR in Fig. 5). According to the Sakhalin Volcanic Eruption Response Team (SVERT), the first signs of an eruption were found in satellite observations acquired on 11 June (Smithsonian, 2007–2011). After the main phase ended on the 16 June, several weaker eruptions occurred in the following 2 weeks. In Fig. 12a, the plume for the combined

**Systematic investigation of BrO in volcanic plumes with GOME-2**

C. Hörmann et al.

Title Page

Abstract

Introduction

Conclusions

References

Tables

Figures

⏪

⏩

◀

▶

Back

Close

Full Screen / Esc

Printer-friendly Version

Interactive Discussion



---

**Systematic investigation of BrO in volcanic plumes with GOME-2**C. Hörmann et al.

---

[Title Page](#)[Abstract](#)[Introduction](#)[Conclusions](#)[References](#)[Tables](#)[Figures](#)[⏪](#)[⏩](#)[◀](#)[▶](#)[Back](#)[Close](#)[Full Screen / Esc](#)[Printer-friendly Version](#)[Interactive Discussion](#)

altitude. The multitude of explosions also points out the difficulties of the determination of a mean BrO/SO<sub>2</sub> ratio for such major eruptions, as several overlapping plumes at different altitudes (and therefore different ambient conditions) might be present in the observed satellite data, which only represent a 2-dimensional projection of the plumes at different altitudes. Additionally, the plume's chemical composition may change significantly in the course of an eruption. In case of the example shown in Fig. 12, we used the starting time of the five strongest explosions within the two days prior to the satellite measurements for the calculation of the forward trajectories (19:00 UTC on 14 June; 1 and 9–11 UTC on 15 June), all of them with reported top heights of more than 10 km. The trajectories for all explosions were calculated for starting heights between 5–20 km at the location of the volcano until the GOME-2 measurements around 00:00 UTC on 16 June. The resulting trajectory endpoints for the time of the GOME-2 observation can be seen in Fig. 13b and agree very well with the overall extent of the detected volcanic plume. Apparently, the plume's transport in opposite directions from the volcano results from different injection heights and a change in the wind direction from westerly to easterly between 11–13 km height. In Fig. 13c, d, the trajectory endpoints are additionally shown in comparison with the SCDs\* of the combined SO<sub>2</sub> product as well as for BrO. A closer look to the trajectory endpoints reveals that the enhanced BrO SCDs\* were most probably caused by the 3 explosions between 9–11 UTC on the 15 June at plume heights of 6–8 km. This indicates, that meteorological parameters such as temperature and relative humidity might have a crucial influence on the formation of BrO in different layers of a volcanic plume in addition to plume conditions such as the individual amount of reactive bromine species and the presence of aerosol particles.

## 5 Systematic analysis of BrO events in volcanic plumes

In order to quantify the abundance of BrO in a more systematic way, we analysed the results from all captured volcanic plumes and divided them into different categories, each one representing a different class of BrO to SO<sub>2</sub> relationship (see Table 3).



**Systematic investigation of BrO in volcanic plumes with GOME-2**

C. Hörmann et al.

[Title Page](#)[Abstract](#)[Introduction](#)[Conclusions](#)[References](#)[Tables](#)[Figures](#)[⏪](#)[⏩](#)[◀](#)[▶](#)[Back](#)[Close](#)[Full Screen / Esc](#)[Printer-friendly Version](#)[Interactive Discussion](#)

In total, 64 individual volcanic plumes were found with indications for the presence of volcanic BrO of which all corresponding maps of the categorised events are available in the attached Supplementary Material. By looking at the results, it again becomes clear that each volcanic eruption/degassing event has its own specific circumstances (see also Sects. 4.1–4.6). For a more detailed analysis of the individual plumes, it will be necessary to perform several case studies in the future, taking into account the influence of volcanic ash, the age of the plume and the plume's height distribution with the corresponding meteorological parameters, such as the ambient air temperature and relative humidity. Here, we limit ourselves to a brief overview of the results.

## 5.1 Category I: clear linear correlation

All captured volcanic plumes that showed signs for a clear linear BrO to SO<sub>2</sub> correlation by a correlation coefficient  $r^2 > 0.5$ , a corresponding p-value  $< 5 \times 10^{-3}$  and a maximum BrO VCD\*  $> 2\sigma^*$  were collected in category I. Additionally, the results were restricted to plume events that contained a cluster of at least 3 neighbouring satellite pixels with BrO VCDs\*  $> 2\sigma^*$ . Table 4 lists the 17 volcanic events that were identified as part of category I, containing individual plumes from 6–8 different volcanoes. Apart from the eruptions that were already discussed in Sect. 4 (Bezymianny, Etna and Kasatochi), plumes from eruptions of Mt. Redoubt and Eyjafjallajökull were identified. Additionally, another plume from an eruption of Etna at the end of November 2007 and two further eruptions on Kamchatka were detected. Like for the already discussed case of the Bezymianny volcano (event No. 22 in Table 4 – see Sect. 4.2), we cannot be completely sure if the named volcanoes were really responsible for the detected volcanic plumes. In case of the Kliuchevskoi eruption on 29/30 March 2011 (event No. 675 in Table 4), the volcanic plume extended over an area of approximately 250 km in latitudinal direction of Kamchatka's eastern coast (encompassing the Kliuchevskoi, Kizimen and Shiveluch volcanoes). While Bezymianny showed no increased activity, the Kizimen volcano (about 100 km south) and the Shiveluch volcano (approximately 80 km north-east) had periods of significant unrest, as reported by KVERT. The location of the

maximum SO<sub>2</sub> SCDs\* and an additional report from the Volcanic Ash Advisory Center Tokyo (VAAC Tokyo) about a possible eruption from Kliuchevskoi on the 30 March indicate, that the major part of the volcanic plume most probably came from Kliuchevskoi (Smithsonian, 2007–2011). For the volcanic plume events over Kamchatka on 8/9 May 2011 (event No. 700 in Table 4) and 7 June 2011 (event No. 740 in Table 4), none of the activity reports from the KVERT can give a clear preference regarding the responsible volcano, but the location of the main parts of the plumes as seen by the OMI instrument indicate that the corresponding eruptions occurred more likely at Kizimen than at the Shiveluch volcano, which also showed increased activity at the same time. For almost all of the category I cases, it is obvious that BrO of volcanic origin was present in the plume, as the BrO SCDs\* were clearly enhanced in the area of enhanced SO<sub>2</sub>. For most cases, the BrO columns even showed a quite similar spatial pattern compared to the SO<sub>2</sub> SCDs\*, indicating a direct one-to-one correlation between the two species. However, it should be pointed out that the presence of enhanced BrO is not that clear for the volcanic plumes of the Ambrym volcano (event No. 535 and No. 563 in Table 4) in comparison to the other events in this category. Figure 14a shows the SO<sub>2</sub> plume from a strong degassing event of Ambrym on 8 April 2010. While the captured SO<sub>2</sub> plume consists only of a few satellite pixels (but can be clearly seen in the map), the BrO map shows no increased values at first sight, since all BrO SCDs\* appear randomly scattered in the whole regarded area (Fig. 14c). This point of view changes by looking only at the area of captured SO<sub>2</sub> plume pixels (Fig. 14b, d). Although the BrO SCDs\* in the plume's area are not well above the SCDs\* in the reference area, a similar pattern can be seen in the distribution of the two species. The correlation plot (Fig. 14e) yields a surprisingly clear linear correlation, with  $r^2 = 0.7$  and a relatively high mean BrO/SO<sub>2</sub> ratio of  $3.3 \times 10^{-4}$ . While the  $r^2$  in this example is one of the highest of all events in category I, it is worth noting that it is also the event with the lowest measured maximum BrO SCD\*. The example therefore demonstrates, that the algorithm seems to be capable to detect relatively low BrO columns produced by a strongly degassing volcano.

**Systematic investigation of BrO in volcanic plumes with GOME-2**

C. Hörmann et al.

Title Page

Abstract

Introduction

Conclusions

References

Tables

Figures

⏪

⏩

◀

▶

Back

Close

Full Screen / Esc

Printer-friendly Version

Interactive Discussion



## 5.2 Category II: weak linear correlation

In category II, all captured volcanic plumes that showed a weak linear BrO to SO<sub>2</sub> correlation were collected. The events in this category were characterized by a correlation coefficient  $0.25 \geq r^2 < 0.5$ , a corresponding p-value  $< 1 \times 10^{-3}$  (80 % lower than in category I) and a maximum BrO VCD\*  $> 2\sigma^*$  (see Table 5). Like for the first category, the results were restricted to plume events that showed a cluster of at least 3 neighbouring satellite pixels with BrO VCDs\*  $> 2\sigma^*$ . For category II, in total 23 different volcanic events from 8–9 different volcanoes were identified. Some days during the eruptions of the highlighted volcanoes in Fig. 5 were detected (Kasatochi, Mt. Redoubt, Eyjafjallajökull and Nabro), but also plumes from eruptions on Kamchatka (Kliuchevskoi, Kizimen and Karymsky). However, the corresponding volcanoes for all plumes could easily be identified due to reports about specific explosion events shortly before the satellite measurements. In addition to several days during the eruptions of Mt. Redoubt and Eyjafjallajökull, also the third day after the eruption of Kasatochi was sorted into category II. Like in the examples in Sect. 4.5, the patterns of the enhanced BrO slant column densities look similar compared to those of SO<sub>2</sub>, but a clear linear correlation between the two species is not found.

## 5.3 Category III: non-linear BrO/SO<sub>2</sub> relation

For the third category, the captured volcanic events were also investigated for plumes without signs of a linear correlation between SO<sub>2</sub> and BrO, but for which significantly enhanced BrO SCDs\* were detected (correlation coefficient  $r^2 \leq 0.25$ ). As no clear linear relationship is found for these cases, the threshold for the maximum BrO VCD\* was increased to  $4\sigma^*$ , in order to assure an unambiguous detection of enhanced BrO in volcanic plumes. Additionally, the cluster size of neighbouring satellite pixels with BrO VCDs\*  $> 2\sigma^*$  (which is the criterion to identify a possible volcanic BrO plume) was raised from 3 to 6.

### Systematic investigation of BrO in volcanic plumes with GOME-2

C. Hörmann et al.

Title Page

Abstract

Introduction

Conclusions

References

Tables

Figures

⏪

⏩

◀

▶

Back

Close

Full Screen / Esc

Printer-friendly Version

Interactive Discussion



## Systematic investigation of BrO in volcanic plumes with GOME-2

C. Hörmann et al.

Title Page

Abstract

Introduction

Conclusions

References

Tables

Figures

⏪

⏩

◀

▶

Back

Close

Full Screen / Esc

Printer-friendly Version

Interactive Discussion



The identified plumes of category III can be seen in Table 6. In total 24 different volcanic events from 6 volcanoes were identified. For this category, only volcanic events were detected that had conspicuously high maximum BrO VCDs<sub>max</sub><sup>\*</sup> in comparison to the SO<sub>2</sub> VCDs<sub>max</sub><sup>\*</sup> in Fig. 5 (Kasatochi, Dalaffilla, Mt. Redoubt, Sarychev, Eyjafjallajökull and Nabro). As already pointed out for the examples in Sects. 4.3–4.6 (Figs. 8–12), most of these events only showed a roughly similar spatial pattern for both of the observed volcanic species. Especially for the eruptions of Kasatochi, Sarychev and Nabro, BrO could only be detected in some parts of the SO<sub>2</sub> plume for these volcanic events, resulting in low  $r^2$  values from the linear fit. Besides the different plume ages and ambient conditions in the different parts of the plume, this might also be caused by the significant ash content that was present during these eruptions and the associated heterogeneous chemical processes in the plume. For some of the detected events, the BrO SCDs<sup>\*</sup> remain quite noisy, although the 6-neighbouring pixels criterion was fulfilled in parts of the plume. This is especially true for the second day after the Dalaffilla eruption (event No. 250 in Table 6), one day of the Mt. Redoubt eruption (event No. 326) and some days during the eruption of Eyjafjallajökull (event No. 559, No. 560 and No. 569). In case of the Nabro eruption, the BrO SCDs<sup>\*</sup> in the area of the captured SO<sub>2</sub> plume were well above the SCDs<sup>\*</sup> in the corresponding reference area, but in contradiction to all other major eruptions, they could only be observed in the area close to the volcano for all detected days, where also the largest SO<sub>2</sub> SCDs<sup>\*</sup> were detected (see Sect. 4.4). For the last 2 detected days of the Nabro eruption in June 2011, the location of the maximum SO<sub>2</sub> SCDs<sup>\*</sup> from the combined SO<sub>2</sub> product (see also Sect. 3.5) matches the one for the maximum BrO SCDs<sup>\*</sup>, which was not the case when using the SO<sub>2</sub> SR.

### 5.4 Category IV: volcanic plumes showing no enhanced BrO SCDs<sup>\*</sup>

The majority of all captured plumes (92 %) showed no signs for the presence of volcanic BrO in the data, i.e. the retrieved BrO SCDs<sup>\*</sup> were not enhanced with respect to the slant columns in the associated reference areas. This resulted in a correlation coefficient  $r^2$  and a BrO/SO<sub>2</sub> ratio close to zero in such cases (the ratio was typically in the

order of  $< 10^{-5}$  for such events). Figure 15 shows such an example for the eruption of the Fernandina volcano (Galapagos Island, Ecuador) on 13 April 2009. In Fig. 15a and c, the background corrected SCDs\* for  $\text{SO}_2$  and BrO are shown, including all pixels of the PEB cluster and the surrounding reference area. Accordingly, Fig. 15b and d show only the identified plume pixels for both species. The resulting correlation plot for the captured plume pixels (Fig. 15e) indicates no enhancement of BrO inside the plume.

## 6 Discussion

Volcanic plumes were systematically extracted from the GOME-2 dataset during the time period between January 2007 and June 2011 (1642 days) by using  $\text{SO}_2$  as a tracer for the plumes' extent. In total, 772 plumes on 553 days (34 % of all regarded days) could be detected in the data, caused by at least 37 different volcanoes. The subsequent analysis of the associated BrO SCDs within the  $\text{SO}_2$  plumes demonstrates the capability of the GOME-2 instrument to monitor the abundance of volcanic BrO during moderate and major eruptions (or even very strong degassing events, whenever the BrO SCD is sufficiently high to exceed the instrument's detection limit). Overall, 64 volcanic plumes from 11–12 different volcanoes were found to show clear evidence for BrO of volcanic origin, which are about 8 % of all captured plumes and about 30 % of all volcanoes which emitted detectable  $\text{SO}_2$  plumes. For at least 6 volcanoes (Dalaffilla, Karymsky, Kizimen, Kliuchevskoi, Nabro and Sarychev) these are the first reported measurements of BrO to the authors' knowledge. Another detected BrO plume can most probably be assigned to the Bezymianny volcano on Kamchatka (event #22; see Sect. 4.2), and three more identified volcanic BrO plumes (events #675, #700 and #740) might have been caused by explosions at the Shiveluch volcano (Kamchatka), although reports from KVERT in combination with OMI data suggest that Kliuchevskoi and Kizimen were most probably the origin of the detected plumes. This demonstrates clearly the advantage of satellite observations to monitor volcanic events in sparsely populated areas, where ground-based measurements are often difficult to realize (e.g.

### Systematic investigation of BrO in volcanic plumes with GOME-2

C. Hörmann et al.

Title Page

Abstract

Introduction

Conclusions

References

Tables

Figures



Back

Close

Full Screen / Esc

Printer-friendly Version

Interactive Discussion



for Dalaffilla in Ethiopia or Nabro in Eritrea). For all other detected BrO plumes, the results confirm the general abundance of BrO at the corresponding volcanoes (Ambrym, Eyjafjallajökull, Kasatochi, Mt. Redoubt) as it has been found from former ground-based, airborne or satellite observations during recent years.

The total number of volcanoes where BrO has been detected by using UV-DOAS measurements, can therefore be raised from 12 to 19 (for a survey of all former BrO observations see Kelly et al., 2012, and references therein).

It is important to point out that cases without significantly enhanced BrO SCDs can be caused by two different reasons:

1. The emissions of quiescent degassing volcanoes and/or during minor eruptions are too low. In such cases even if moderate or high BrO/SO<sub>2</sub> ratios are present in the plume, the BrO SCDs will be below the detection limit.
2. The BrO/SO<sub>2</sub> ratio is too low. This might be even the case for moderate or strong eruptions with high SO<sub>2</sub> SCDs. Regarding the top five of all 772 volcanic plumes with the largest SO<sub>2</sub> SCDs\* in this study, two of them showed no evidence for the presence of volcanic BrO (Merapi on 5 November 2010 with a maximum SO<sub>2</sub> SCDs\* of  $8.9 \times 10^{18}$ , respectively Grímsvötn on 22 May 2011 with a maximum SO<sub>2</sub> SCDs\* of  $2.2 \times 10^{19}$  molecule cm<sup>-2</sup>). However, from such cases, upper limits for the BrO/SO<sub>2</sub> ratio can be estimated by the ratio of the maximum BrO and SO<sub>2</sub> SCDs\* or the resulting slope of the linear fit (both ratios can be found in the Supplementary Material for all investigated plumes). For the above mentioned cases of Merapi and Grímsvötn, the upper limits for the BrO/SO<sub>2</sub> ratios were found to be  $8 \times 10^{-6}$  and  $2.5 \times 10^{-6}$ , respectively.

Since satellite instruments usually have a relatively large footprint (40 × 80 km<sup>2</sup> for GOME-2), they are not able to resolve small scale variations in the trace gas distribution. All measured columns of SO<sub>2</sub> and BrO need therefore to be interpreted as mean values within the area of a satellite pixel. This also implies that significantly higher BrO

**Systematic investigation of BrO in volcanic plumes with GOME-2**

C. Hörmann et al.

Title Page

Abstract

Introduction

Conclusions

References

Tables

Figures

⏪

⏩

◀

▶

Back

Close

Full Screen / Esc

Printer-friendly Version

Interactive Discussion



and SO<sub>2</sub> SCDs and probably also BrO/SO<sub>2</sub> ratios might have been present locally in the highlighted volcanic plumes.

## 6.1 Different BrO/SO<sub>2</sub> relationships

The collected examples of volcanic plumes show large variations of the BrO/SO<sub>2</sub> behaviour. For some of the identified plumes, the extent and shape of the BrO plume is roughly comparable to that of SO<sub>2</sub> and is accompanied by a similar distribution of the two species within the plume. This results in high values for the correlation coefficient ( $r^2 > 0.5$ ) for the respective SCDs of the extracted plume pixels and allows us to determine the mean BrO/SO<sub>2</sub> ratio. Most of these cases were observed for moderate eruptions, where a well-defined compact plume was visible in the satellite data less than 24 h after the start of the associated eruption.

For other cases, only a weak linear correlation between BrO and SO<sub>2</sub> columns was observed that on the one hand may be caused by BrO SCDs that were only slightly above the instrument's detection limit, and on the other hand possibly due to the gradual chemical processing of aged volcanic plumes. For instance, in parts of the plume of the Dalaffilla eruption (Sect. 4.3), BrO was well correlated with SO<sub>2</sub>, whereas in other parts no BrO was found. One explanation for this behaviour might be that not only the local composition of the volcanic plume (such as ash and/or other plume contents) have a crucial influence on the formation of BrO but that the ambient meteorological conditions (temperature, relative humidity and plume height) also play an important role. This is also suggested by the results for the Sarychev eruption (see Sect. 4.6), where enhanced BrO SCDs were only observed in relative low plume heights of 6–8 km, but not at higher altitudes (> 10 km), even if the largest SO<sub>2</sub> SCDs occurred here. The HYSPLIT trajectory analysis of the Sarychev case points out another problem that may show up especially during major eruptions. Passive DOAS instruments, such as GOME-2, SCIAMACHY and OMI often can not distinguish volcanic plumes at different altitude, but that overlap in the x-y-plane of observation. To investigate the influence of different ambient conditions on the formation of BrO in individual parts of the detected

### Systematic investigation of BrO in volcanic plumes with GOME-2

C. Hörmann et al.

Title Page

Abstract

Introduction

Conclusions

References

Tables

Figures



Back

Close

Full Screen / Esc

Printer-friendly Version

Interactive Discussion





volcanic plumes, further trajectory calculations along with chemical model simulations will be necessary. Such simulations might be also used in order to analyse the temporal development of the BrO/SO<sub>2</sub> ratio and determine the lifetime for both species. This will be essential for the calculation of total SO<sub>2</sub> and BrO budgets in the future.

## 6.2 Comparison to previous ground-based measurements

It should be emphasized that comparisons of satellite observations with ground-based measurements have to be interpreted with care, as they almost exclusively detect plumes from explosive eruptions, whereas ground-based observations usually investigate stable conditions at degassing volcanoes. Ground-based observations of volcanic plumes are ideal for the investigation of the initial development of the BrO/SO<sub>2</sub> behaviour during the first minutes after the plume's release at quiescent degassing volcanoes, but the advantage of satellite instruments like GOME-2, SCIAMACHY and OMI lies in the ability to investigate this behaviour in entire volcanic plumes from moderate/major eruptions or strong degassing events on a much larger spatial and temporal scale. Nevertheless our results indicate that the BrO/SO<sub>2</sub> ratios during eruptions and periods of quiet degassing are not significantly different, as the BrO/SO<sub>2</sub> ratios for all identified volcanic BrO events were found to be similar to the ones from worldwide ground-based measurements with some 10<sup>-5</sup> to several 10<sup>-4</sup> (for a survey of former BrO observations the reader is again referred to Kelly et al., 2012, and references therein).

## 6.3 Comparison to previous satellite studies

An attempt to investigate the abundance of volcanic BrO using GOME and SCIAMACHY data by Afe et al. (2004) failed. As the spatial resolution of SCIAMACHY is better than for the GOME-2 instrument (30 × 60 km<sup>2</sup> compared to 40 × 80 km<sup>2</sup>), this result appears surprising. Meanwhile, the SCIAMACHY instrument has proven to be

### Systematic investigation of BrO in volcanic plumes with GOME-2

C. Hörmann et al.

Title Page

Abstract

Introduction

Conclusions

References

Tables

Figures



Back

Close

Full Screen / Esc

Printer-friendly Version

Interactive Discussion



able to detect enhanced BrO SCDs of volcanic origin as well, as the BrO plume from Kasatochi was clearly visible in the data (Theys et al., 2009).

In order to further investigate the potential of SCIAMACHY to detect BrO during volcanic events, we looked at BrO Level-2 data from the Belgian Institute for Space Aeronomy (Van Roozendaal et al., 2006b) for all volcanic plumes with enhanced BrO SCDs that we had found in the GOME-2 data within this study (see Tables 4, 5 and 6). A considerable fraction of the identified plume areas with enhanced BrO SCDs (36 %) was not covered by the SCIAMACHY instrument. Especially for the major eruptions of Sarychev and Nabro, the instrument missed the affected plume regions for almost all days, as the enhanced BrO columns occurred only in a relatively small area of about  $10^\circ \times 10^\circ$ , while the gaps in SCIAMACHY observations are typically  $4^\circ \times 15^\circ$  in latitude and longitude, respectively. For all other volcanic plumes, the SCIAMACHY data indeed showed similar enhancements of the BrO SCDs in 90 % of these cases. Only for about 10 % of these events, the enhanced BrO columns were not clearly visible in the SCIAMACHY data, even though the instrument provided a sufficient coverage of the volcanic plume. However, in those cases the BrO SCDs were also close to the detection limit of the GOME-2 measurements.

The poor daily coverage of the instrument in combination with the comparatively short time period of about 18 months of SCIAMACHY data (33 scenes of volcanic  $\text{SO}_2$  emissions from August 2002–January 2004) that were analysed in Afe et al. (2004) might be the main reason why their attempt failed. However, some of the proposed explanations for the lack of correlation between  $\text{SO}_2$  and BrO columns in Afe et al. (2004) remain plausible and important, particularly because for the majority of GOME-2 measurements in the here presented study, no evidence for volcanic BrO was found either. The most important reasons are:

1. Current satellite instruments are usually not sensitive enough for the detection of BrO from steadily degassing volcanoes, especially not on daily basis. This is, for a large part, due to the coarse spatial resolution of these instruments, as a single ground pixel may cover an area that is much larger than the plume, causing the

---

**Systematic investigation of BrO in volcanic plumes with GOME-2**C. Hörmann et al.

---

Title Page

Abstract

Introduction

Conclusions

References

Tables

Figures

⏪

⏩

◀

▶

Back

Close

Full Screen / Esc

Printer-friendly Version

Interactive Discussion



**Systematic investigation of BrO in volcanic plumes with GOME-2**

C. Hörmann et al.

[Title Page](#)[Abstract](#)[Introduction](#)[Conclusions](#)[References](#)[Tables](#)[Figures](#)[⏪](#)[⏩](#)[◀](#)[▶](#)[Back](#)[Close](#)[Full Screen / Esc](#)[Printer-friendly Version](#)[Interactive Discussion](#)

already small BrO SCDs to decrease. In most cases, only larger BrO plumes from moderate to major eruptions are detected. Furthermore, the sensitivity of satellite measurements decreases towards lower altitudes.

2. The formation rate and lifetime of BrO is influenced by several factors, like the plume height and the associated ambient meteorological conditions, the plume's composition and also probably the abundance of volcanic ash, which has an important influence on heterogeneous chemistry. While clearly enhanced BrO SCDs were for example detected after the Kasatochi eruption for several days thousands of kilometres from the volcano, this was only possible for a few hundred kilometres and approximately a plume age of 24 h after the eruption of the Nabro volcano.
3. The fraction of halogen compounds of volcanic emissions and thus the amount of reactive halogen compounds in volcanic plumes may vary for individual volcanoes, so that the reactive bromine content for some of the space monitored eruptions is insufficient to form detectable amounts of BrO. Furthermore, the geo-physical processes inside a volcano, such as the different solubility of bromine and sulphur in the melt depending on the movements of magma, might also play an important role for the initial BrO/SO<sub>2</sub> ratio during an eruption, as it was recently suggested by Bobrowski and Giuffrida (2012). Examples for very low BrO/SO<sub>2</sub> ratios are the major eruptions of Okmok (July 2008), Merapi (October/November 2010) and Grímsvötn (May 2011), with estimated upper limits in the range of 10<sup>-6</sup> to 10<sup>-5</sup>.

## 7 Conclusions

We have systematically investigated the GOME-2 dataset from January 2007 until June 2011 for the abundance of bromine monoxide in volcanic plumes. 772 plumes that were caused by enhanced volcanic activity and/or eruptions of about 37 different volcanoes have been extracted from the data by using SO<sub>2</sub> as a tracer. In total, 64 volcanic plumes

from 11–12 different volcanoes (and therefore about one third of all observed volcanoes) showed clear evidence for the formation of BrO after the plumes' release (8 % of all captured plumes). For the volcanoes of Dalaffilla, Karymsky, Kizimen, Kliuchevskoi, Bezymianny, Nabro and Sarychev, these are the first reported measurements of BrO to the authors' knowledge and therefore raise the total number of volcanoes where BrO has been detected from 12 to 19.

Corresponding BrO/SO<sub>2</sub> ratios for all cases of enhanced BrO SCDs were found to be similar to worldwide ground-based measurements that usually investigate stable conditions at quiescent degassing volcanoes. Although the majority of the detected volcanic plumes originated from explosive eruptions, the BrO/SO<sub>2</sub> ratios were of the same order of magnitude, ranging from some 10<sup>-5</sup> to several 10<sup>-4</sup>. However, the majority of all investigated volcanic plumes (92 %) showed no evidence for the abundance of BrO, even for eruptions with very high SO<sub>2</sub> SCDs like the ones of Merapi and Grímsvötn. Here, the corresponding BrO/SO<sub>2</sub> ratios have been estimated to were below 8 × 10<sup>-6</sup> and 2.5 × 10<sup>-6</sup>, respectively.

While some of the extracted volcanic plumes showed a good correlation of the SO<sub>2</sub> and BrO distribution patterns, others revealed only a similar enhancement of BrO in parts of the plume or even only a roughly similar spatial pattern. One explanation for this behaviour might be that not only the local composition of the volcanic plume (such as ash and/or other plume contents) has a crucial influence on the formation of BrO but that also the ambient meteorological conditions (e.g. temperature and relative humidity) play an important role. A detailed analysis of these conditions (especially the accurate determination of plume altitudes with the help of trajectory calculations) along with chemical model simulations are therefore crucial in order to further investigate the involved chemical mechanisms.

In the future, a detailed analysis of higher spatially resolved OMI data (available since October 2004 up to now with full daily global coverage) and the re-analysis of the entire SCIAMACHY data for the last 10 yr will probably increase the total number of volcanic BrO observations. In addition, the GOME-2 series will be completed by two additional

**Systematic investigation of BrO in volcanic plumes with GOME-2**

C. Hörmann et al.

Title Page

Abstract

Introduction

Conclusions

References

Tables

Figures



Back

Close

Full Screen / Esc

Printer-friendly Version

Interactive Discussion



instruments during the next 5–10 yr and provide further data in order to improve the spatial coverage and temporal resolution of volcanic monitoring from space. Furthermore, the Sentinel satellite series of the European Space Agency (ESA) will provide instruments with much higher spatial and temporal resolution for atmospheric monitoring (Sentinel-5 and Sentinel-5 precursor) and even one high resolution instrument on a geostationary satellite (Sentinel-4).

**Supplementary material related to this article is available online at:**  
[http://www.atmos-chem-phys-discuss.net/12/29325/2012/  
acpd-12-29325-2012-supplement.pdf](http://www.atmos-chem-phys-discuss.net/12/29325/2012/acpd-12-29325-2012-supplement.pdf).

*Acknowledgements.* The authors gratefully acknowledge Kornelia Mies and Rüdiger Sörensen from MPIC Mainz for technical support on the GOME-2 data. This work has been financially supported by the International Max Planck Research School for Atmospheric Chemistry and Physics, Mainz (Germany).

The service charges for this open access publication have been covered by the Max Planck Society.

## References

- Afe, O. T., Richter, A., Sierk, B., Wittrock, F., and Burrows, J. P.: BrO emission from volcanoes: a survey using GOME and SCIAMACHY measurements, *Geophys. Res. Lett.*, 31, L24113, doi:10.1029/2004GL020994, 2004. 29328, 29340, 29357, 29358
- Bani, P., Oppenheimer, C., Tsanev, V., Carn, S., Cronin, S., Crimp, R., Calkins, J., Charley, D., Lardy, M., and Roberts, T.: Surge in sulphur and halogen degassing from Ambrym volcano, Vanuatu, *B. Volcanol.*, 71, 1159–1168, doi:10.1007/s00445-009-0293-7, 2009. 29327
- Barrie, L. A., Bottenheim, J. W., Schnell, R. C., Crutzen, P. J., and Rasmussen, R. A.: Ozone destruction and photochemical reactions at polar sunrise in the lower Arctic atmosphere, *Nature*, 334, 138–141, doi:10.1038/334138a0, 1988. 29326

29361

ACPD

12, 29325–29389, 2012

## Systematic investigation of BrO in volcanic plumes with GOME-2

C. Hörmann et al.

Title Page

Abstract

Introduction

Conclusions

References

Tables

Figures

⏪

⏩

◀

▶

Back

Close

Full Screen / Esc

Printer-friendly Version

Interactive Discussion



## Systematic investigation of BrO in volcanic plumes with GOME-2

C. Hörmann et al.

[Title Page](#)
[Abstract](#)
[Introduction](#)
[Conclusions](#)
[References](#)
[Tables](#)
[Figures](#)
[Back](#)
[Close](#)
[Full Screen / Esc](#)
[Printer-friendly Version](#)
[Interactive Discussion](#)


Bobrowski, N. and Giuffrida, G.: Bromine monoxide/sulphur dioxide ratios in relation to volcanological observations at Mt. Etna 2006–2009, *Solid Earth Discuss.*, 4, 475–505, doi:10.5194/sed-4-475-2012, 2012. 29328, 29359

Bobrowski, N. and Platt, U.: SO<sub>2</sub>/BrO ratios studied in five volcanic plumes, *J. Volcanol. Geoth. Res.*, 166, 147–160, doi:10.1016/j.jvolgeores.2007.07.003, 2007. 29327

Bobrowski, N., Hönniger, G., Galle, B., and Platt, U.: Detection of bromine monoxide in a volcanic plume, *Nature*, 423, 273–276, doi:10.1038/nature01625, 2003. 29327, 29346

Bobrowski, N., von Glasow, R., Aiuppa, A., Inguaggiato, S., Louban, I., Ibrahim, O. W., and Platt, U.: Reactive halogen chemistry in volcanic plumes, *J. Geophys. Res.*, 112, D06311, doi:10.1029/2006JD007206, 2007. 29327, 29328

Bobrowski, N., Kern, C., Platt, U., Hörmann, C., and Wagner, T.: Novel SO<sub>2</sub> spectral evaluation scheme using the 360–390 nm wavelength range, *Atmos. Meas. Tech.*, 3, 879–891, doi:10.5194/amt-3-879-2010, 2010. 29332

Bogumil, K., Orphal, J., Homann, T., Voigt, S., Spietz, P., Fleischmann, O., Vogel, A., Hartmann, M., Kromminga, H., Bovensmann, H., Frerick, J., and Burrows, J.: Measurements of molecular absorption spectra with the SCIAMACHY pre-flight model: instrument characterization and reference data for atmospheric remote-sensing in the 230–2380 nm region, *J. Photoch. Photobio. A*, 157, 167–184, doi:10.1016/S1010-6030(03)00062-5, 2003. 29331, 29332

Boichu, M., Oppenheimer, C., Roberts, T. J., Tsanev, V., and Kyle, P. R.: On bromine, nitrogen oxides and ozone depletion in the tropospheric plume of Erebus volcano (Antarctica), *Atmos. Environ.*, 45, 3856–3866, doi:10.1016/j.atmosenv.2011.03.027, 2011. 29327

Bonaccorso, A., Bonforte, A., Calvari, S., Negro, C. D., Grazia, G. D., Ganci, G., Neri, M., Vicari, A., and Boschi, E.: The initial phases of the 2008–2009 Mount Etna eruption: a multidisciplinary approach for hazard assessment, *J. Geophys. Res.*, 116, B03203, doi:10.1029/2010JB007906, 2011. 29343

Bovensmann, H., Burrows, J. P., Buchwitz, M., Frerick, J., Noël, S., Rozanov, V. V., Chance, K. V., and Goede, A. P. H.: SCIAMACHY: mission objectives and measurement modes, *J. Atmos. Sci.*, 56, 127–150, doi:10.1175/1520-0469(1999)056<0127:SMOAMM>2.0.CO;2, 1999. 29329

Brenninkmeijer, C. A. M., Crutzen, P., Boumard, F., Dauer, T., Dix, B., Ebinghaus, R., Filippi, D., Fischer, H., Franke, H., Frieß, U., Heintzenberg, J., Helleis, F., Hermann, M., Kock, H. H., Koepfel, C., Lelieveld, J., Leuenberger, M., Martinsson, B. G., Miemczyk, S., Moret, H. P.,

## Systematic investigation of BrO in volcanic plumes with GOME-2

C. Hörmann et al.

Title Page

Abstract

Introduction

Conclusions

References

Tables

Figures

⏪

⏩

◀

▶

Back

Close

Full Screen / Esc

Printer-friendly Version

Interactive Discussion



Nguyen, H. N., Nyfeler, P., Oram, D., O'Sullivan, D., Penkett, S., Platt, U., Pupek, M., Ramonet, M., Randa, B., Reichelt, M., Rhee, T. S., Rohwer, J., Rosenfeld, K., Scharffe, D., Schlager, H., Schumann, U., Slemr, F., Sprung, D., Stock, P., Thaler, R., Valentino, F., van Velthoven, P., Waibel, A., Wandel, A., Waschitschek, K., Wiedensohler, A., Xueref-Remy, I., Zahn, A., Zech, U., and Ziereis, H.: Civil Aircraft for the regular investigation of the atmosphere based on an instrumented container: The new CARIBIC system, *Atmos. Chem. Phys.*, 7, 4953–4976, doi:10.5194/acp-7-4953-2007, 2007. 29329

Callies, J., Corpaccioli, E., Eisinger, M., Hahne, A., and Lefevre, A.: GOME-2 – MetOp's second generation sensor for operational ozone monitoring, *ESA Bull.*, 102, 28–36, 2000. 29331

Cantrell, C. A.: Technical Note: Review of methods for linear least-squares fitting of data and application to atmospheric chemistry problems, *Atmos. Chem. Phys.*, 8, 5477–5487, doi:10.5194/acp-8-5477-2008, 2008. 29342

De Smedt, I., Van Roozendael, M., and Jacobs, T.: Technical Note: Optimization of DOAS Settings for BrO Fitting from SCIAMACHY Nadir Spectra – Comparison with GOME BrO Retrievals, Belgian Institute for Space Aeronomy (IASB-BIRA), Brussels, Belgium, 2004. 29329

Dikty, S. and Richter, A.: GOME-2 on MetOp-A Support for Analysis of GOME-2 In-Orbit Degradation and Impacts on Level 2 Data Products, final report, October 2011, available at: [http://www.eumetsat.int/groups/ops/documents/document/pdf\\_gome2\\_degrade\\_final\\_rep.pdf](http://www.eumetsat.int/groups/ops/documents/document/pdf_gome2_degrade_final_rep.pdf), last access: 12 September 2012, 2011. 29337

Draxler, R. R. and Rolph, G. D.: HYSPLIT (HYbrid Single-Particle Lagrangian Integrated Trajectory) model access via NOAA ARL READY Website, available at: <http://ready.arl.noaa.gov/HYSPLIT.php>, last access: 12 September 2012, 2012. 29348

EUMETSAT: GOME-2 Product Guide, available at: <http://oiswww.eumetsat.org/WEBOPS/eps-pg/GOME-2/GOME2-PG-index.htm>, last access: 12 September 2012, 2005. 29331

Fan, S. and Jacob, D. J.: Surface ozone depletion in Arctic spring sustained by bromine reactions on aerosols, *Nature*, 359, 522–524, doi:10.1038/359522a0, 1992. 29328

Galle, B., Bobrowski, N., Carn, S., Johansson, M., Kasereka, M., Oppenheimer, C., Yalire, M., and Zhang, Y.: Gas Emissions from Nyiragongo Volcano, D.R. of Congo, measured by UV Mini-DOAS Spectroscopy, EGU meeting, available at: <http://www.cosis.net/abstracts/EGU05/08332/EGU05-J-08332.pdf>, last access: 12 September 2012, 2005. 29327

Gerlach, T. M.: Volcanic sources of tropospheric ozone-depleting trace gases, *Geochem. Geophys. Geosy.*, 5, Q09007, doi:10.1029/2004GC000747, 2004. 29327



## Systematic investigation of BrO in volcanic plumes with GOME-2

C. Hörmann et al.

[Title Page](#)
[Abstract](#)
[Introduction](#)
[Conclusions](#)
[References](#)
[Tables](#)
[Figures](#)
[⏪](#)
[⏩](#)
[◀](#)
[▶](#)
[Back](#)
[Close](#)
[Full Screen / Esc](#)
[Printer-friendly Version](#)
[Interactive Discussion](#)


- Graaf, M. D., Stammes, P., Torres, O., and Koelemeijer, R. B. A.: Absorbing aerosol index: sensitivity analysis, application to GOME and comparison with TOMS, *J. Geophys. Res.*, 110, D01201, doi:10.1029/2004JD005178, 2005. 29348
- Graf, H., Feichter, J., and Langmann, B.: Volcanic sulfur emissions: estimates of source strength and its contribution to the global sulfate distribution, *J. Geophys. Res.*, 102, 10727–10738, doi:199710.1029/96JD03265, 1997. 29327
- Greenblatt, G. D., Orlando, J. J., Burkholder, J. B., and Ravishankara, A. R.: Absorption measurements of oxygen between 330 and 1140 nm, *J. Geophys. Res.*, 95, 18577–18582, doi:199010.1029/JD095iD11p18577, 1997. 29332
- Gür, B., Spietz, P., Orphal, J., and Burrows, J. P.: Absorption Spectra Measurements with the GOME-2 FMs Using the IUP/IFE-UBs Calibration Apparatus for Trace Gas Absorption Spectroscopy VATGAS, Final Report, University of Bremen, October 2005, 2005. 29331, 29332
- Herman, J. R., Bhartia, P. K., Torres, O., Hsu, C., Sefstor, C., and Celarier, E.: Global distribution of UV-absorbing aerosols from Nimbus 7/TOMS data, *J. Geophys. Res.*, 102, 16911–16922, doi:199710.1029/96JD03680, 1997. 29348
- Heue, K.-P., Brenninkmeijer, C. A. M., Baker, A. K., Rauthe-Schöch, A., Walter, D., Wagner, T., Hörmann, C., Sihler, H., Dix, B., Frieß, U., Platt, U., Martinsson, B. G., van Velthoven, P. F. J., Zahn, A., and Ebinghaus, R.: SO<sub>2</sub> and BrO observation in the plume of the Eyjafjallajökull volcano 2010: CARIBIC and GOME-2 retrievals, *Atmos. Chem. Phys.*, 11, 2973–2989, doi:10.5194/acp-11-2973-2011, 2011. 29327, 29329, 29338
- Kelly, P. J., Kern, C., Roberts, T. J., Lopez, T., Werner, C., and Aiuppa, A.: Rapid chemical evolution of tropospheric volcanic emissions from Redoubt Volcano, Alaska, based on observations of ozone and halogen-containing gases, *J. Volcanol. Geoth. Res.*, doi:10.1016/j.jvolgeores.2012.04.023, in press, 2012. 29327, 29355, 29357
- Kern, C., Vogel, L., Rivera, C., Herrera, M., Platt, U., and Sihler, H.: Halogen oxide measurements at Masaya Volcano, Nicaragua using active long path differential optical absorption spectroscopy, *B. Volcanol.*, 71, 659–670, doi:10.1007/s00445-008-0252-8, 2008. 29328
- Levin, B. W., Rybin, A. V., Vasilenko, N. F., Prytkov, A. S., Chibisova, M. V., Kogan, M. G., Steblov, G. M., and Frolov, D. I.: Monitoring of the eruption of the Sarychev Peak Volcano in Matua Island in 2009 (Central Kurile Islands), *Dokl. Earth Sci.*, 435, 1507–1510, doi:10.1134/S1028334X10110218, 2010. 29348

**Systematic investigation of BrO in volcanic plumes with GOME-2**

C. Hörmann et al.

Title Page

Abstract

Introduction

Conclusions

References

Tables

Figures

◀

▶

◀

▶

Back

Close

Full Screen / Esc

Printer-friendly Version

Interactive Discussion



- Louban, I., Bobrowski, N., Rouwet, D., Inguaggiato, S., and Platt, U.: Imaging DOAS for volcanological applications, *B. Volcanol.*, 71, 753–765, doi:10.1007/s00445-008-0262-6, 2009. 29328
- 5 McConnell, J. C., Henderson, G. S., Barrie, L., Bottenheim, J., Niki, H., Langford, C. H., and Templeton, E. M. J.: Photochemical bromine production implicated in Arctic boundary-layer ozone depletion, *Nature*, 355, 150–152, doi:10.1038/355150a0, 1992. 29328
- Munro, R., Eisinger, M., Anderson, C., Callies, J., Carpaccioli, E., Lang, R., Lefevre, A., Livschitz, Y., and Albinana, A. P.: GOME-2 on MetOp, in: *The 2006 EUMETSAT Meteorological Satellite Conference*, 12–16 June 2006, Helsinki, Finland, 2006. 29331
- 10 Neal, C. A., McGimsey, R. G., Dixon, J. P., Cameron, C. E., Nuzhaev, A. A., and Chibisova, M.: 2008 Volcanic Activity in Alaska, Kamchatka, and the Kurile Islands: Summary of Events and Response of the Alaska Volcano Observatory: U.S. Geological Survey Scientific Investigations Report 2010-5243, available at: <http://pubs.usgs.gov/sir/2010/5243>, last access: 12 September 2012, 2011. 29346
- 15 Oppenheimer, C., Tsanev, V., Braban, C., Cox, R., Adams, J., Aiuppa, A., Bobrowski, N., Delmelle, P., Barclay, J., and Mcgonigle, A.: BrO formation in volcanic plumes, *Geochim. Cosmochim. Ac.*, 70, 2935–2941, doi:10.1016/j.gca.2006.04.001, 2006. 29327
- Penning de Vries, M. J. M., Beirle, S., and Wagner, T.: UV Aerosol Indices from SCIAMACHY: introducing the Sattering Index (SCI), *Atmos. Chem. Phys.*, 9, 9555–9567, doi:10.5194/acp-9-9555-2009, 2009. 29348
- 20 Platt, U. and Lehrer, E.: Arctic Tropospheric Ozone Chemistry, ARCTOC, Final Report of the EU-Project No. EV5V-CT93-0318, Heidelberg, 1996. 29328
- Platt, U. and Stutz, J.: *Differential Optical Absorption Spectroscopy: Principles And Applications*, Springer, Berlin, Heidelberg, 2008. 29331
- 25 Richter, A.: Algorithm Theoretical Basis Document for the GOME-2 Rapid Volcanic SO<sub>2</sub> Product, first draft, October 2009, available at: [http://www.doas-bremen.de/so2.alerts/gome2\\_so2\\_atbd\\_091005.pdf](http://www.doas-bremen.de/so2.alerts/gome2_so2_atbd_091005.pdf), last access: 12 September 2012, 2009. 29334
- Richter, A., Wittrock, F., Ladstätter-Weissenmayer, A., and Burrows, J. P.: GOME measurements of stratospheric and tropospheric BrO, *Adv. Space Res.*, 29, 1667–1672, doi:10.1016/S0273-1177(02)00123-0, 2002. 29328
- 30 Richter, A., Wittrock, F., Schönhardt, A., and Burrows, J.: Quantifying Volcanic SO<sub>2</sub> Emissions Using GOME-2 Measurements, Poster at the EGU General Assembly 2009, 7679, XY247,

## Systematic investigation of BrO in volcanic plumes with GOME-2

C. Hörmann et al.

Title Page

Abstract

Introduction

Conclusions

References

Tables

Figures

⏪

⏩

◀

▶

Back

Close

Full Screen / Esc

Printer-friendly Version

Interactive Discussion



available at: [http://www.iup.uni-bremen.de/doas/posters/egu\\_2009\\_richter.pdf](http://www.iup.uni-bremen.de/doas/posters/egu_2009_richter.pdf), last access: 12 September 2012, 2009. 29332

Rix, M., Valks, P., Hao, N., Loyola, D., Schlager, H., Huntrieser, H., Flemming, J., Koehler, U., Schumann, U., and Inness, A.: Volcanic SO<sub>2</sub>, BrO and plume height estimations using GOME-2 satellite measurements during the eruption of Eyjafjallajökull in May 2010, *J. Geophys. Res.*, 117, D00U19, doi:10.1029/2011JD016718, 2012. 29330

Rolph, G. D.: Real-time Environmental Applications and Display sYstem (READY) Website, available at: <http://ready.arl.noaa.gov>, last access: 12 September 2012, 2012. 29348

SACS: Support to Aviation Control Service, available at: <http://sacs.aeronomie.be>, last access: 12 September 2012, 2012. 29334, 29345

Sihler, H., Platt, U., Beirle, S., Marbach, T., Kühl, S., Dörner, S., Verschaeve, J., Frieß, U., Pöhler, D., Vogel, L., Sander, R., and Wagner, T.: Tropospheric BrO column densities in the Arctic from satellite: retrieval and comparison to ground-based measurements, *Atmos. Meas. Tech. Discuss.*, 5, 3199–3270, doi:10.5194/amtd-5-3199-2012, 2012. 29332

Simpson, W. R., von Glasow, R., Riedel, K., Anderson, P., Ariya, P., Bottenheim, J., Burrows, J., Carpenter, L. J., Frieß, U., Goodsite, M. E., Heard, D., Hutterli, M., Jacobi, H.-W., Kaleschke, L., Neff, B., Plane, J., Platt, U., Richter, A., Roscoe, H., Sander, R., Shepson, P., Sodeau, J., Steffen, A., Wagner, T., and Wolff, E.: Halogens and their role in polar boundary-layer ozone depletion, *Atmos. Chem. Phys.*, 7, 4375–4418, doi:10.5194/acp-7-4375-2007, 2007. 29327, 29328

Smithsonian: Global Volcanism Program, Smithsonian/USGS Weekly Volcanic Activity Reports 2007–2011, available at: <http://volcano.si.edu/reports/usgs/>, last access: 12 September 2012, 2007–2011. 29343, 29344, 29345, 29347, 29351

Textor, C., Graf, H., and Timmreck, C.: Emissions from Volcanoes, vol. 18, edited by: Granier, C., Artaxo, P., Reeves, C. E., Kluwer Academic Publ., Dordrecht, 269–303, 2004. 29330, 29334

Theys, N., Roozendael, M. V., Dils, B., Hendrick, F., Hao, N., and Mazière, M. D.: First satellite detection of volcanic bromine monoxide emission after the Kasatochi eruption, *Geophys. Res. Lett.*, 36, L03809, doi:10.1029/2008GL036552, 2009. 29329, 29346, 29358

Theys, N., Van Roozendael, M., Hendrick, F., Yang, X., De Smedt, I., Richter, A., Begoin, M., Errera, Q., Johnston, P. V., Kreher, K., and De Mazière, M.: Global observations of tropospheric BrO columns using GOME-2 satellite data, *Atmos. Chem. Phys.*, 11, 1791–1811, doi:10.5194/acp-11-1791-2011, 2011. 29328

**Systematic  
investigation of BrO  
in volcanic plumes  
with GOME-2**

C. Hörmann et al.

Title Page

Abstract

Introduction

Conclusions

References

Tables

Figures

◀

▶

◀

▶

Back

Close

Full Screen / Esc

Printer-friendly Version

Interactive Discussion



Torres, O., Bhartia, P. K., Herman, J. R., Ahmad, Z., and Gleason, J.: Derivation of aerosol properties from satellite measurements of backscattered ultraviolet radiation: theoretical basis, *J. Geophys. Res.*, 103, 17099–17110, doi:199810.1029/98JD00900, 1998. 29348

5 Van Roozendael, M., Loyola, D., Spurr, R., Balis, D., Lambert, J., Livschitz, Y., Valks, P., Rupert, T., Kenter, P., Fayt, C., and Zehner, C.: Ten years of GOME/ERS-2 total ozone data—the new GOME data processor (GDP) version 4: 1. algorithm description, *J. Geophys. Res.*, 111, D14311, doi:10.1029/2005JD006375, 2006a. 29331

10 Van Roozendael, M., Theys, N., and De Smedt, I.: SCIAMACHY BrO total column Product Specification Document, rev. 1, 30 January 2006, available at: [http://bro.aeronomie.be/Documents/BIRA\\_SCIA\\_BrO\\_PSD\\_v1r1.pdf](http://bro.aeronomie.be/Documents/BIRA_SCIA_BrO_PSD_v1r1.pdf), the data is freely available at <http://bro.aeronomie.be/level2.php>, last access: 12 September 2012, 2006b. 29358

Vandaele, A. C., Hermans, C., Fally, S., Carleer, M., Colin, R., Mérienne, M., Jenouvrier, A., and Coquart, B.: High-resolution Fourier transform measurement of the NO<sub>2</sub> visible and near-infrared absorption cross sections: temperature and pressure effects, *J. Geophys. Res.*, 107, 4348, doi:10.1029/2001JD000971, 2002. 29332

15 von Glasow, R.: Atmospheric chemistry in volcanic plumes, *P. Natl. Acad. Sci. USA*, 107, 6594–6599, doi:10.1073/pnas.0913164107, 2010. 29327, 29328

von Glasow, R. and Crutzen, P.: Tropospheric halogen chemistry, in: *Treatise on Geochemistry*, Elsevier, Oxford, 1–67, 2003. 29327, 29328

20 Wagner, T. and Platt, U.: Satellite mapping of enhanced BrO concentrations in the troposphere, *Nature*, 395, 486–490, doi:10.1038/26723, 1998. 29328, 29339

Wagner, T., Beirle, S., and Deutschmann, T.: Three-dimensional simulation of the Ring effect in observations of scattered sun light using Monte Carlo radiative transfer models, *Atmos. Meas. Tech.*, 2, 113–124, doi:10.5194/amt-2-113-2009, 2009. 29331

25 Wennberg, P.: Atmospheric chemistry: bromine explosion, *Nature*, 397, 299–301, doi:10.1038/16805, 1999. 29328

Wilmouth, D. M., Hanisco, T. F., Donahue, N. M., and Anderson, J. G.: Fourier transform ultraviolet spectroscopy of the A  $2\pi 3/2 \leftarrow X 2\pi 3/2$  Transition of BrO, *J. Phys. Chem. A*, 103, 8935–8945, doi:10.1021/jp991651o, 1999. 29332

30 Yang, K., Krotkov, N. A., Krueger, A. J., Carn, S. A., Bhartia, P. K., and Levelt, P. F.: Retrieval of large volcanic SO<sub>2</sub> columns from the Aura Ozone Monitoring Instrument: comparison and limitations, *J. Geophys. Res.*, 112, D24S43, doi:10.1029/2007JD008825, 2007. 29332

Yang, K., Liu, X., Krotkov, N. A., Krueger, A. J., and Carn, S. A.: Estimating the altitude of volcanic sulfur dioxide plumes from space borne hyper-spectral UV measurements, Geophys. Res. Lett., 36, L10803, doi:10.1029/2009GL038025, 2009. 29332

---

**Systematic  
investigation of BrO  
in volcanic plumes  
with GOME-2**

C. Hörmann et al.

---

Title Page

Abstract

Introduction

Conclusions

References

Tables

Figures



Back

Close

Full Screen / Esc

Printer-friendly Version

Interactive Discussion



## Systematic investigation of BrO in volcanic plumes with GOME-2

C. Hörmann et al.

Title Page

Abstract

Introduction

Conclusions

References

Tables

Figures

◀

▶

◀

▶

Back

Close

Full Screen / Esc

Printer-friendly Version

Interactive Discussion



**Table 1.** Areas where the GOME-2 data were excluded for the automatic detection of volcanic SO<sub>2</sub> plumes. The first three areas are affected by anthropogenic emissions of SO<sub>2</sub>, whereas erroneous signals are detected over large parts of South America, where the deformation of Earth's magnetic field allows cosmic high-energy particles to create false signals in the detector of the satellite instrument (South Atlantic Anomaly).

Name	Reason	Excluded area
Highveld plateau	Anthropogenic emissions	[20–35° S, 20–35° E]
China	Anthropogenic emissions	[20–45° N, 100–135° E] [30–50° N, 130–140° E]
Norilsk	Anthropogenic emissions	[50–70° N, 70–110° E] [60–70° N, 65–70° E]
South Atlantic Anomaly (SAA)	Cosmic particles	[10–70° S, 10–85° W] [0–10° S, 10–75° W] [20–35° S, 0–10° W]

## Systematic investigation of BrO in volcanic plumes with GOME-2

C. Hörmann et al.

**Table 2.** Examples for the abundance of volcanic BrO that are presented in Sects. 4.1–4.6.

label	volcano	date	section	figure
ET	Etna	14 May 2008	Sect. 4.1	Fig. 6
BZ	Bezymianny	11/12 May 2007	Sect. 4.2	Fig. 7
DL	Dalaffilla	4 Nov 2007	Sect. 4.3	Fig. 8
NB	Nabro	16 Jun 2011	Sect. 4.4	Fig. 9
KS	Kasatochi	9 and 11 Aug 2008	Sect. 4.5	Figs. 10–11
SR	Sarychev	15/16 Jun 2009	Sect. 4.6	Fig. 12

Title Page

Abstract

Introduction

Conclusions

References

Tables

Figures

⏪

⏩

◀

▶

Back

Close

Full Screen / Esc

Printer-friendly Version

Interactive Discussion



## Systematic investigation of BrO in volcanic plumes with GOME-2

C. Hörmann et al.

**Table 3.** Categories that were used for the BrO/SO<sub>2</sub> analysis of all detected volcanic plumes.

Category	Description	$r^2$	p-value	BrO VCD* <sub>max</sub>	BrO cluster	Number of events
I	Clear linear BrO/SO <sub>2</sub> correlation	> 0.5	< 5 × 10 <sup>-3</sup>	> 2σ*	3-pixel cluster with VCD* > 2σ*	17
II	Weak linear BrO/SO <sub>2</sub> correlation	≥ 0.25	< 1 × 10 <sup>-3</sup>	> 2σ*	3-pixel cluster with VCD* > 2σ*	23
III	Non-linear BrO/SO <sub>2</sub> relation	≤ 0.25	–	> 4σ*	6-pixel cluster with VCD* > 2σ*	24
IV	No enhanced BrO	–	–	–	–	708

[Title Page](#)
[Abstract](#)
[Introduction](#)
[Conclusions](#)
[References](#)
[Tables](#)
[Figures](#)
[Back](#)
[Close](#)
[Full Screen / Esc](#)
[Printer-friendly Version](#)
[Interactive Discussion](#)


## Systematic investigation of BrO in volcanic plumes with GOME-2

C. Hörmann et al.

**Table 4. Category I (clear linear correlation).** BrO/SO<sub>2</sub>-analysis of all detected volcanic plumes of Category I. Columns contain: event number, volcano, measurement date, max. BrO SCD, max. SO<sub>2</sub> SCD, coincidence of max. SO<sub>2</sub> and BrO SCD, correlation coefficient, BrO/SO<sub>2</sub> slope, ratio of max. SO<sub>2</sub> and BrO SCD and coordinates of regarded area.

#	Volcano	Date	BrO SCD <sub>max</sub> [molecule cm <sup>-2</sup> ]	SO <sub>2</sub> SCD <sub>max</sub> [molecule cm <sup>-2</sup> ]	L <sup>b</sup>	r <sup>2</sup>	BrO/SO <sub>2</sub> slope	BrO <sub>max</sub> / SO <sub>2max</sub>	Coordinates
22	Bezymianny <sup>d</sup>	11/12 May 2007	1.3 × 10 <sup>14</sup>	3.1 × 10 <sup>17</sup>	no	0.62	4.4 × 10 <sup>-4</sup>	4.1 × 10 <sup>-4</sup>	[40–70° N, 145–180° E]
68 <sup>c</sup>	Etna	24 Nov 2007	1.4 × 10 <sup>14</sup>	1.1 × 10 <sup>18</sup>	yes	0.61	1.0 × 10 <sup>-4</sup>	1.2 × 10 <sup>-4</sup>	[20–49° N, 0–35° E]
94 <sup>a</sup>	Etna	11 May 2008	2.3 × 10 <sup>14</sup>	1.5 × 10 <sup>18</sup>	yes	0.60	9.8 × 10 <sup>-5</sup>	1.4 × 10 <sup>-4</sup>	[20–55° N, 5–45° E]
97	Etna	14 May 2008	2.4 × 10 <sup>14</sup>	8.2 × 10 <sup>17</sup>	yes	0.70	2.5 × 10 <sup>-4</sup>	2.9 × 10 <sup>-4</sup>	[20–60° N, –5–35° E]
164 <sup>a</sup>	Kasatochi	11 Aug 2008	3.7 × 10 <sup>14</sup>	1.9 × 10 <sup>19</sup>	no	0.50	4.2 × 10 <sup>-5</sup>	1.9 × 10 <sup>-5</sup>	[20–70° N, 60–180° W]
282 <sup>a</sup>	Mt. Redoubt	26 Mar 2009	1.9 × 10 <sup>14</sup>	5.8 × 10 <sup>18</sup>	yes	0.90	3.5 × 10 <sup>-5</sup>	3.3 × 10 <sup>-5</sup>	[40–70° N, 135–170° W]
322	Mt. Redoubt	18 Apr 2009	1.1 × 10 <sup>14</sup>	4.8 × 10 <sup>17</sup>	no	0.62	2.2 × 10 <sup>-4</sup>	2.4 × 10 <sup>-4</sup>	[35–70° N, 135–170° W]
363	Mt. Redoubt	29 May 2009	9.1 × 10 <sup>13</sup>	3.8 × 10 <sup>17</sup>	yes	0.56	2.4 × 10 <sup>-4</sup>	2.4 × 10 <sup>-4</sup>	[45–70° N, 135–170° W]
535	Ambrym	8 Apr 2010	6.7 × 10 <sup>13</sup>	3.0 × 10 <sup>17</sup>	no	0.70	3.3 × 10 <sup>-4</sup>	2.2 × 10 <sup>-4</sup>	[0–35° S, 150–185° E]
541	Eyjafjallajökull	23 Apr 2010	1.6 × 10 <sup>14</sup>	3.7 × 10 <sup>17</sup>	yes	0.65	5.1 × 10 <sup>-4</sup>	4.3 × 10 <sup>-4</sup>	[45–70° N, 0–35° W]
545	Eyjafjallajökull	25 Apr 2010	1.3 × 10 <sup>14</sup>	4.6 × 10 <sup>17</sup>	no	0.75	3.3 × 10 <sup>-4</sup>	2.9 × 10 <sup>-4</sup>	[45–70° N, 0–35° W]
546	Eyjafjallajökull	26 Apr 2010	8.8 × 10 <sup>13</sup>	4.2 × 10 <sup>17</sup>	yes	0.58	2.5 × 10 <sup>-4</sup>	2.0 × 10 <sup>-4</sup>	[45–70° N, 0–35° W]
550	Eyjafjallajökull	29 Apr 2010	1.3 × 10 <sup>14</sup>	6.1 × 10 <sup>17</sup>	yes	0.54	1.9 × 10 <sup>-4</sup>	2.1 × 10 <sup>-4</sup>	[40–70° N, 0–45° W]
563	Ambrym	11 May 2010	8.6 × 10 <sup>13</sup>	6.4 × 10 <sup>17</sup>	yes	0.59	1.6 × 10 <sup>-4</sup>	1.3 × 10 <sup>-4</sup>	[0–35° S, 150–190° E]
675	Kliuchevskoi <sup>d</sup>	29/30 Mar 2011	1.3 × 10 <sup>14</sup>	6.0 × 10 <sup>17</sup>	yes	0.79	2.6 × 10 <sup>-4</sup>	2.1 × 10 <sup>-4</sup>	[40–70° N, 145–180° E]
700	Kizimen <sup>d</sup>	8/9 May 2011	8.8 × 10 <sup>13</sup>	3.3 × 10 <sup>17</sup>	no	0.56	3.0 × 10 <sup>-4</sup>	2.6 × 10 <sup>-4</sup>	[40–70° N, 140–180° E]
740	Kizimen <sup>d</sup>	7 Jun 2011	6.8 × 10 <sup>13</sup>	1.6 × 10 <sup>17</sup>	yes	0.63	4.7 × 10 <sup>-4</sup>	4.0 × 10 <sup>-4</sup>	[40–70° N, 145–180° E]

<sup>a</sup> Combined SO<sub>2</sub> product in case of high SO<sub>2</sub> SCDs ≥ 1 × 10<sup>18</sup> [molecule cm<sup>-2</sup>].

<sup>b</sup> Location of SO<sub>2</sub> SCD<sub>max</sub> is the same as for BrO SCD<sub>max</sub>.

<sup>c</sup> SO<sub>2</sub> SCDs ≥ 1 × 10<sup>18</sup> [molecule cm<sup>-2</sup>], but no plume pixels found in the SO<sub>2</sub> AR.

<sup>d</sup> Corresponding volcano cannot be clearly identified.

Title Page

Abstract

Introduction

Conclusions

References

Tables

Figures

⏪

⏩

◀

▶

Back

Close

Full Screen / Esc

Printer-friendly Version

Interactive Discussion



## Systematic investigation of BrO in volcanic plumes with GOME-2

C. Hörmann et al.

Title Page	
Abstract	Introduction
Conclusions	References
Tables	Figures
◀	▶
◀	▶
Back	Close
Full Screen / Esc	
Printer-friendly Version	
Interactive Discussion	

**Table 5. Category II (weak linear correlation).** BrO/SO<sub>2</sub>-analysis of all detected volcanic plumes of Category II. Columns contain: event number, volcano, measurement date, max. BrO SCD, max. SO<sub>2</sub> SCD, coincidence of max. SO<sub>2</sub> and BrO SCD, correlation coefficient, BrO/SO<sub>2</sub> slope, ratio of max. SO<sub>2</sub> and BrO SCD and coordinates of regarded area.

#	Volcano	Date	BrO SCD <sub>max</sub> [molecule cm <sup>-2</sup> ]	SO <sub>2</sub> SCD <sub>max</sub> [molecule cm <sup>-2</sup> ]	L <sup>b</sup>	r <sup>2</sup>	BrO/SO <sub>2</sub> slope	BrO <sub>max</sub> / SO <sub>2max</sub>	Coordinates
28	Kliuchevskoi	20/21 May 2007	5.1 × 10 <sup>13</sup>	1.9 × 10 <sup>17</sup>	no	0.40	2.7 × 10 <sup>-4</sup>	2.6 × 10 <sup>-4</sup>	[40–70° N, 145–180° E]
48	Ambrym	16 Jul 2007	5.3 × 10 <sup>13</sup>	2.6 × 10 <sup>17</sup>	yes	0.38	2.1 × 10 <sup>-4</sup>	2.0 × 10 <sup>-4</sup>	[0–35° S, 150–181° E]
163 <sup>a</sup>	Kasatochi	10 Aug 2008	4.3 × 10 <sup>14</sup>	1.9 × 10 <sup>19</sup>	no	0.41	2.4 × 10 <sup>-5</sup>	2.2 × 10 <sup>-5</sup>	[25–70° N, 110–185° W]
186	Kasatochi	20 Aug 2008	5.0 × 10 <sup>13</sup>	2.8 × 10 <sup>17</sup>	no	0.28	1.6 × 10 <sup>-4</sup>	1.7 × 10 <sup>-4</sup>	[35–70° N, 160–180° W]
278 <sup>a</sup>	Mt. Redoubt	11 Mar 2009	1.7 × 10 <sup>14</sup>	4.4 × 10 <sup>18</sup>	no	0.47	4.4 × 10 <sup>-5</sup>	3.8 × 10 <sup>-5</sup>	[45–70° N, 115–170° W]
279	Mt. Redoubt	24 Mar 2009	1.1 × 10 <sup>14</sup>	1.0 × 10 <sup>18</sup>	no	0.50	1.0 × 10 <sup>-4</sup>	1.0 × 10 <sup>-4</sup>	[45–70° N, 115–142° W]
281	Mt. Redoubt	26 Mar 2009	9.3 × 10 <sup>13</sup>	7.2 × 10 <sup>17</sup>	no	0.31	1.4 × 10 <sup>-4</sup>	1.2 × 10 <sup>-4</sup>	[20–70° N, 85–130° W]
306	Mt. Redoubt	9 Apr 2009	8.5 × 10 <sup>13</sup>	3.3 × 10 <sup>17</sup>	no	0.41	3.0 × 10 <sup>-4</sup>	2.5 × 10 <sup>-4</sup>	[40–70° N, 115–170° W]
312	Mt. Redoubt	13 Apr 2009	9.2 × 10 <sup>13</sup>	3.0 × 10 <sup>17</sup>	no	0.33	2.7 × 10 <sup>-4</sup>	3.0 × 10 <sup>-4</sup>	[45–70° N, 135–170° W]
317	Mt. Redoubt	16 Apr 2009	1.4 × 10 <sup>14</sup>	5.1 × 10 <sup>17</sup>	yes	0.49	2.6 × 10 <sup>-4</sup>	2.7 × 10 <sup>-4</sup>	[35–70° N, 140–180° W]
324	Mt. Redoubt	19 Apr 2009	6.7 × 10 <sup>13</sup>	3.3 × 10 <sup>17</sup>	no	0.33	2.1 × 10 <sup>-4</sup>	2.0 × 10 <sup>-4</sup>	[50–70° N, 140–175° W]
344	Mt. Redoubt	5 May 2009	8.2 × 10 <sup>13</sup>	3.0 × 10 <sup>17</sup>	no	0.37	2.6 × 10 <sup>-4</sup>	2.7 × 10 <sup>-4</sup>	[35–70° N, 140–175° W]
551	Eyjafjallajökull	30 Apr 2010	1.4 × 10 <sup>14</sup>	4.2 × 10 <sup>17</sup>	yes	0.50	2.9 × 10 <sup>-4</sup>	3.3 × 10 <sup>-4</sup>	[40–70° N, –40–5° E]
555	Eyjafjallajökull	5 May 2010	1.7 × 10 <sup>14</sup>	7.2 × 10 <sup>17</sup>	no	0.34	1.3 × 10 <sup>-4</sup>	2.4 × 10 <sup>-4</sup>	[35–70° N, –35–15° E]
557	Eyjafjallajökull	7 May 2010	1.0 × 10 <sup>14</sup>	5.5 × 10 <sup>17</sup>	no	0.29	1.5 × 10 <sup>-4</sup>	1.9 × 10 <sup>-4</sup>	[20–70° N, –45–10° E]
558	Eyjafjallajökull	8 May 2010	9.5 × 10 <sup>13</sup>	5.7 × 10 <sup>17</sup>	no	0.26	1.5 × 10 <sup>-4</sup>	1.6 × 10 <sup>-4</sup>	[25–70° N, 0–50° W]
568	Eyjafjallajökull	14 May 2010	1.3 × 10 <sup>14</sup>	8.4 × 10 <sup>17</sup>	no	0.42	1.4 × 10 <sup>-4</sup>	1.6 × 10 <sup>-4</sup>	[35–70° N, –50–15° E]
570	Eyjafjallajökull	16 May 2010	1.2 × 10 <sup>14</sup>	3.5 × 10 <sup>17</sup>	no	0.32	3.1 × 10 <sup>-4</sup>	3.5 × 10 <sup>-4</sup>	[35–70° N, –35–20° E]
572	Eyjafjallajökull	17 May 2010	1.5 × 10 <sup>14</sup>	7.3 × 10 <sup>17</sup>	no	0.42	2.6 × 10 <sup>-4</sup>	2.0 × 10 <sup>-4</sup>	[35–70° N, –55–20° E]
696	Kizimen	3 May 2011	6.6 × 10 <sup>13</sup>	3.7 × 10 <sup>17</sup>	yes	0.46	2.1 × 10 <sup>-4</sup>	1.7 × 10 <sup>-4</sup>	[40–70° N, 140–175° E]
706	Karymsky	21/22 May 2011	8.0 × 10 <sup>13</sup>	3.7 × 10 <sup>17</sup>	no	0.44	2.1 × 10 <sup>-4</sup>	2.1 × 10 <sup>-4</sup>	[35–70° N, 140–175° E]
748 <sup>a</sup>	Nabro	15 Jun 2011	2.6 × 10 <sup>14</sup>	2.2 × 10 <sup>19</sup>	no	0.27	1.8 × 10 <sup>-5</sup>	1.1 × 10 <sup>-5</sup>	[–10–65° N, 5–95° E]
749 <sup>a</sup>	Nabro	16 Jun 2011	1.8 × 10 <sup>14</sup>	1.2 × 10 <sup>19</sup>	no	0.29	2.0 × 10 <sup>-5</sup>	1.4 × 10 <sup>-5</sup>	[–15–60° N, 0–110° E]

<sup>a</sup> Combined SO<sub>2</sub> product in case of high SO<sub>2</sub> SCDs ≥ 1 × 10<sup>18</sup> [molecule cm<sup>-2</sup>].

<sup>b</sup> Location of SO<sub>2</sub> SCD<sub>max</sub> is the same as for BrO SCD<sub>max</sub>.

## Systematic investigation of BrO in volcanic plumes with GOME-2

C. Hörmann et al.

[Title Page](#)
[Abstract](#)
[Introduction](#)
[Conclusions](#)
[References](#)
[Tables](#)
[Figures](#)
[Back](#)
[Close](#)
[Full Screen / Esc](#)
[Printer-friendly Version](#)
[Interactive Discussion](#)

**Table 6. Category III (eruptions with enhanced BrO cluster, but no linear correlation).** BrO/SO<sub>2</sub>-analysis of all detected volcanic plumes of Category III. Columns contain: event number, volcano, measurement date, max. BrO SCD, max. SO<sub>2</sub> SCD, coincidence of max. SO<sub>2</sub> and BrO SCD, correlation coefficient, BrO/SO<sub>2</sub> slope, ratio of max. SO<sub>2</sub> and BrO SCD and coordinates of regarded area.

#	Volcano	Date	BrO SCD <sub>max</sub> [molecule cm <sup>-2</sup> ]	SO <sub>2</sub> SCD <sub>max</sub> [molecule cm <sup>-2</sup> ]	L <sup>b</sup>	r <sup>2</sup>	BrO/SO <sub>2</sub> slope	BrO <sub>max</sub> / SO <sub>2max</sub>	Coordinates
160 <sup>a</sup>	Kasatochi	8 Aug 2008	3.6 × 10 <sup>14</sup>	3.9 × 10 <sup>19</sup>	no	0.22	8.6 × 10 <sup>-6</sup>	9.2 × 10 <sup>-6</sup>	[30–70° N, 145–195° W]
162 <sup>a</sup>	Kasatochi	9 Aug 2008	4.5 × 10 <sup>14</sup>	2.6 × 10 <sup>19</sup>	no	0.24	1.9 × 10 <sup>-5</sup>	1.7 × 10 <sup>-5</sup>	[25–70° N, 135–190° W]
165 <sup>a</sup>	Kasatochi	12 Aug 2008	3.0 × 10 <sup>14</sup>	1.6 × 10 <sup>19</sup>	no	0.21	2.4 × 10 <sup>-5</sup>	1.9 × 10 <sup>-5</sup>	[20–70° N, 50–175° W]
167 <sup>a</sup>	Kasatochi	13 Aug 2008	1.3 × 10 <sup>14</sup>	1.5 × 10 <sup>19</sup>	no	0.14	1.2 × 10 <sup>-5</sup>	9.0 × 10 <sup>-6</sup>	[25–70° N, 20–175° W]
169 <sup>a</sup>	Kasatochi	14 Aug 2008	1.1 × 10 <sup>14</sup>	6.9 × 10 <sup>18</sup>	no	0.00	1.8 × 10 <sup>-6</sup>	1.7 × 10 <sup>-5</sup>	[20–70° N, –200–15° E]
249 <sup>a</sup>	Dalaffilla	4 Nov 2008	1.7 × 10 <sup>14</sup>	4.3 × 10 <sup>18</sup>	no	0.01	1.4 × 10 <sup>-5</sup>	3.9 × 10 <sup>-5</sup>	[0–40° N, 30–70° E]
250 <sup>a</sup>	Dalaffilla	5 Nov 2008	1.2 × 10 <sup>14</sup>	1.6 × 10 <sup>18</sup>	no	0.05	3.1 × 10 <sup>-5</sup>	7.4 × 10 <sup>-5</sup>	[–5–50° N, 25–100° E]
280	Mt. Redoubt	25 Mar 2009	1.2 × 10 <sup>14</sup>	1.0 × 10 <sup>18</sup>	no	0.25	8.2 × 10 <sup>-5</sup>	1.2 × 10 <sup>-4</sup>	[30–70° N, 100–140° W]
326	Mt. Redoubt	20 Apr 2009	9.1 × 10 <sup>13</sup>	4.2 × 10 <sup>17</sup>	no	0.17	2.2 × 10 <sup>-4</sup>	2.1 × 10 <sup>-4</sup>	[40–70° N, 135–170° W]
369 <sup>a</sup>	Sarychev	12/13 Jun 2009	1.2 × 10 <sup>14</sup>	1.7 × 10 <sup>18</sup>	no	0.02	2.2 × 10 <sup>-5</sup>	7.0 × 10 <sup>-5</sup>	[30–65° N, 130–175° E]
370 <sup>a</sup>	Sarychev	13/14 Jun 2009	1.0 × 10 <sup>14</sup>	3.9 × 10 <sup>18</sup>	no	0.01	4.6 × 10 <sup>-6</sup>	2.7 × 10 <sup>-5</sup>	[25–70° N, 115–235° W]
375 <sup>a</sup>	Sarychev	15/16 Jun 2009	1.9 × 10 <sup>14</sup>	2.3 × 10 <sup>19</sup>	no	0.01	3.9 × 10 <sup>-6</sup>	8.2 × 10 <sup>-6</sup>	[25–70° N, 120–180° E]
377 <sup>a</sup>	Sarychev	16/17 Jun 2009	1.4 × 10 <sup>14</sup>	1.6 × 10 <sup>19</sup>	no	0.01	4.0 × 10 <sup>-6</sup>	8.7 × 10 <sup>-6</sup>	[20–70° N, 135–250° W]
378 <sup>a</sup>	Sarychev	17/18 Jun 2009	1.6 × 10 <sup>14</sup>	1.1 × 10 <sup>19</sup>	no	0.01	5.8 × 10 <sup>-6</sup>	1.4 × 10 <sup>-5</sup>	[20–70° N, 115–250° W]
380 <sup>a</sup>	Sarychev	19 Jun 2009	1.4 × 10 <sup>14</sup>	2.3 × 10 <sup>18</sup>	no	0.02	8.7 × 10 <sup>-6</sup>	6.3 × 10 <sup>-5</sup>	[45–70° N, 110–135° E]
548	Eyjafjallajökull	27 Apr 2010	1.1 × 10 <sup>14</sup>	3.1 × 10 <sup>17</sup>	no	0.07	9.4 × 10 <sup>-5</sup>	3.5 × 10 <sup>-4</sup>	[45–70° N, 0–40° W]
559	Eyjafjallajökull	09 May 2010	1.0 × 10 <sup>14</sup>	5.0 × 10 <sup>17</sup>	no	0.14	1.3 × 10 <sup>-4</sup>	2.1 × 10 <sup>-4</sup>	[25–70° N, –55–5° E]
560	Eyjafjallajökull	10 May 2010	9.8 × 10 <sup>13</sup>	3.8 × 10 <sup>17</sup>	no	0.12	1.1 × 10 <sup>-4</sup>	2.5 × 10 <sup>-4</sup>	[20–70° N, –50–5° E]
569	Eyjafjallajökull	15 May 2010	8.8 × 10 <sup>13</sup>	4.4 × 10 <sup>17</sup>	no	0.02	4.6 × 10 <sup>-5</sup>	2.0 × 10 <sup>-4</sup>	[40–70° N, 0–60° W]
745 <sup>a</sup>	Nabro	13 Jun 2011	2.6 × 10 <sup>14</sup>	1.0 × 10 <sup>19</sup>	no	0.00	3.0 × 10 <sup>-6</sup>	2.4 × 10 <sup>-5</sup>	[–5–35° N, 10–60° E]
755 <sup>a</sup>	Nabro	20 Jun 2011	1.4 × 10 <sup>14</sup>	5.6 × 10 <sup>18</sup>	no	0.12	3.2 × 10 <sup>-5</sup>	2.6 × 10 <sup>-5</sup>	[–20–55° N, –13–130° E]
758 <sup>a</sup>	Nabro	21 Jun 2011	1.5 × 10 <sup>14</sup>	5.2 × 10 <sup>18</sup>	no	0.08	2.7 × 10 <sup>-5</sup>	2.9 × 10 <sup>-5</sup>	[–25–55° N, –15–90° E]
760 <sup>a</sup>	Nabro	22 Jun 2011	1.1 × 10 <sup>14</sup>	3.8 × 10 <sup>18</sup>	yes	0.11	3.6 × 10 <sup>-5</sup>	3.0 × 10 <sup>-5</sup>	[–20–50° N, –20–100° E]
767 <sup>a</sup>	Nabro	26 Jun 2011	1.2 × 10 <sup>14</sup>	3.6 × 10 <sup>18</sup>	yes	0.27	4.2 × 10 <sup>-5</sup>	3.3 × 10 <sup>-5</sup>	[–10–55° N, –4–75° E]

<sup>a</sup> Combined SO<sub>2</sub> product in case of high SO<sub>2</sub> SCDs ≥ 1 × 10<sup>18</sup> [molecule cm<sup>-2</sup>].

<sup>b</sup> Location of SO<sub>2</sub> SCD<sub>max</sub> is the same as for BrO SCD<sub>max</sub>.

## Systematic investigation of BrO in volcanic plumes with GOME-2

C. Hörmann et al.

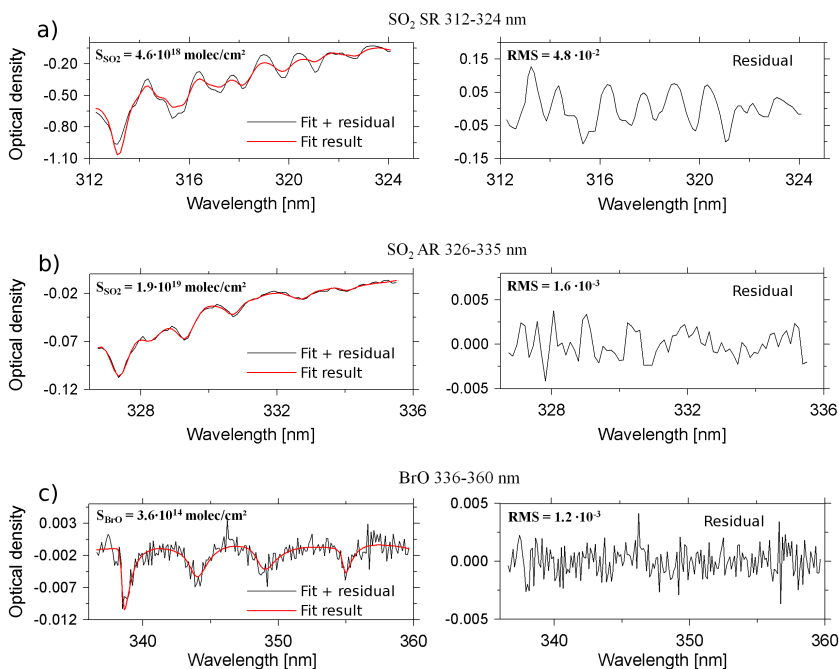


**Fig. 1.** Example of all three fit-scenarios, **(a)** SO<sub>2</sub> standard retrieval 312.1–324 nm, **(b)** SO<sub>2</sub> alternative retrieval 326.5–335.3 nm, **(c)** BrO retrieval 336–360 nm, for a GOME-2 pixel in the volcanic plume of Kasatochi on 9 August 2008 (21:05 UTC, centre coordinates 160.01° W 46.87° N). Left column: fit results including the residual (black lines) and reference spectra (red lines) scaled according to the fit results (the resulting SCD ( $S$ ) and root mean square (RMS) is also noted). Right column: corresponding residuals (please note expanded scales).

[Title Page](#)
[Abstract](#)
[Introduction](#)
[Conclusions](#)
[References](#)
[Tables](#)
[Figures](#)
[⏪](#)
[⏩](#)
[◀](#)
[▶](#)
[Back](#)
[Close](#)
[Full Screen / Esc](#)
[Printer-friendly Version](#)
[Interactive Discussion](#)

## Systematic investigation of BrO in volcanic plumes with GOME-2

C. Hörmann et al.

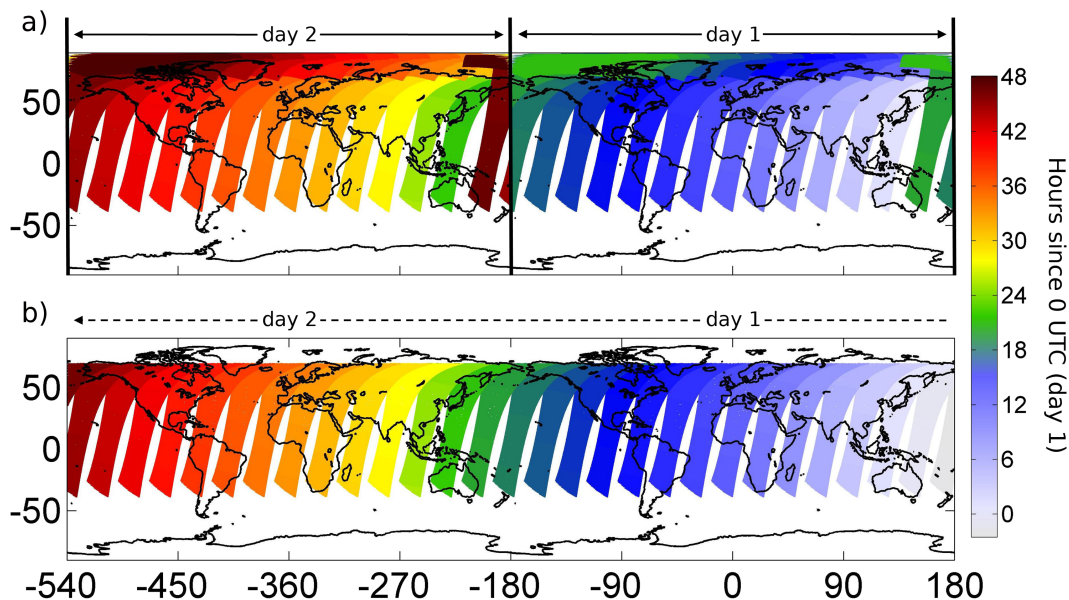


**Fig. 2.** (a) Two consecutive daily maps of GOME-2 satellite orbits as widely used in the scientific community (right: day 1, left: day 2). Due to an overlap of the first and the last orbit during one regarded day (area between light blue and green orbit for day 1 and green and dark red orbits during day 2), a temporal discontinuity of up to more than 24 h occurs. Additionally, overlapping pixels at high latitudes show a time shift of up to  $\sim 10$  h and another time shift of  $\sim 24$  h occurs at the intersecting region between day 1 and day 2. (b) Alternative global map layout for the maps with two days coverage. The chronology of satellite orbits in direct succession is now conserved in westerly direction. Measurements at more than  $\pm 70^\circ$  N and neighbouring pixels with a time shift  $> 3.5$  h are also filtered out.

Title Page

Abstract

Introduction

Conclusions

References

Tables

Figures

◀

▶

◀

▶

Back

Close

Full Screen / Esc

Printer-friendly Version

Interactive Discussion

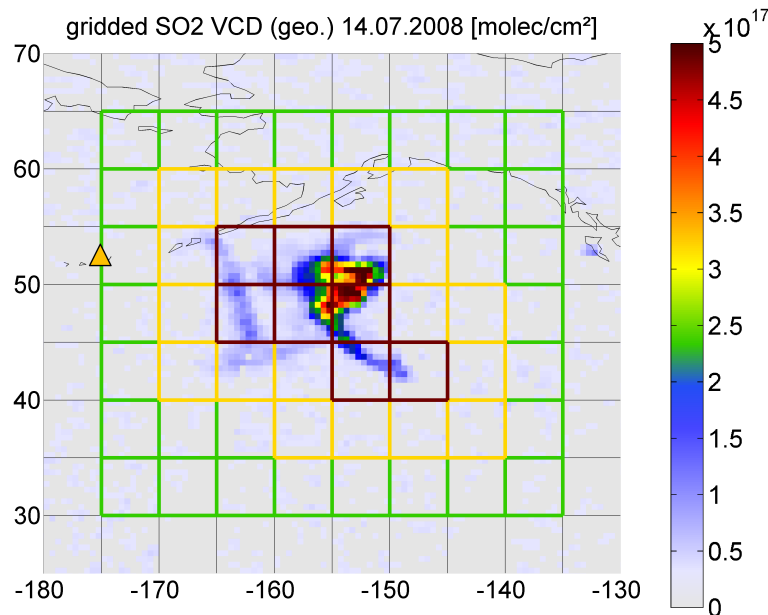


**Fig. 3.** Automatic detection of the volcanic SO<sub>2</sub> plume after the eruption of the Okmok volcano (orange triangle) on 14 July 2008. The red frames in the centre region highlight the detected SO<sub>2</sub> plume event boxes (PEBs) that were identified to contain parts of the volcanic plume. Neighbouring boxes are assigned to each specific PEB in order to capture also those parts of the volcanic plume where the VCDs were not sufficiently high to be identified as an individual PEB (yellow boxes). Finally, in order to get a reference area next to the captured SO<sub>2</sub> plume events, all non-SO<sub>2</sub> PEBs within another surrounding box that exceeded from  $\pm 5^\circ$  from the max/min latitudinal/longitudinal grid pixel position of the SO<sub>2</sub> PEB cluster were registered (green boxes).

**Systematic investigation of BrO in volcanic plumes with GOME-2**

C. Hörmann et al.

Title Page	
Abstract	Introduction
Conclusions	References
Tables	Figures
◀	▶
◀	▶
Back	Close
Full Screen / Esc	
Printer-friendly Version	
Interactive Discussion	





## Systematic investigation of BrO in volcanic plumes with GOME-2

C. Hörmann et al.

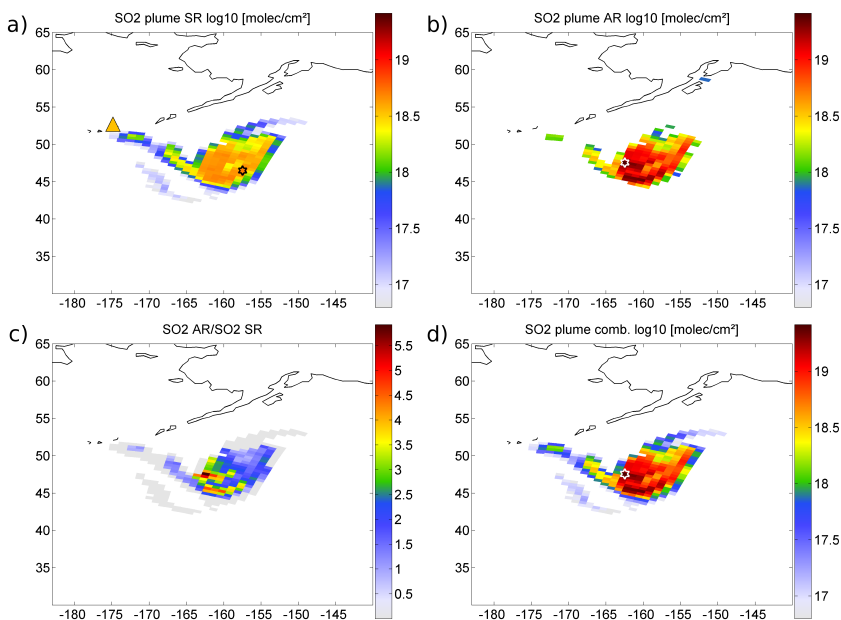


**Fig. 4.** Volcanic  $\text{SO}_2$  plume as seen by GOME-2 on 9 August 2008 during the eruption of Kasatochi volcano. **(a)**  $\text{SO}_2$  SCDs from the standard retrieval (312.1–324 nm), **(b)**  $\text{SO}_2$  SCDs from the alternative retrieval (326.5–335.3 nm). While the maximum  $\text{SO}_2$  SCD for the SR ( $5.2 \times 10^{18}$  molecule  $\text{cm}^{-2}$ ) is located in the south-eastern part of the plume (indicated by a black hexagon), it is now found to be shifted towards the west with a 5 times higher SCD ( $2.7 \times 10^{19}$  molecule  $\text{cm}^{-2}$ ) in the AR (white hexagon). **(c)** Ratios between the  $\text{SO}_2$  SCDs from the alternative and standard retrieval **(d)** The new  $\text{SO}_2$  SCD product combines the results from both retrievals. Note the logarithmic scale in **(a)**, **(b)** and **(d)**.

Title Page

Abstract

Introduction

Conclusions

References

Tables

Figures

◀

▶

◀

▶

Back

Close

Full Screen / Esc

Printer-friendly Version

Interactive Discussion

## Systematic investigation of BrO in volcanic plumes with GOME-2

C. Hörmann et al.

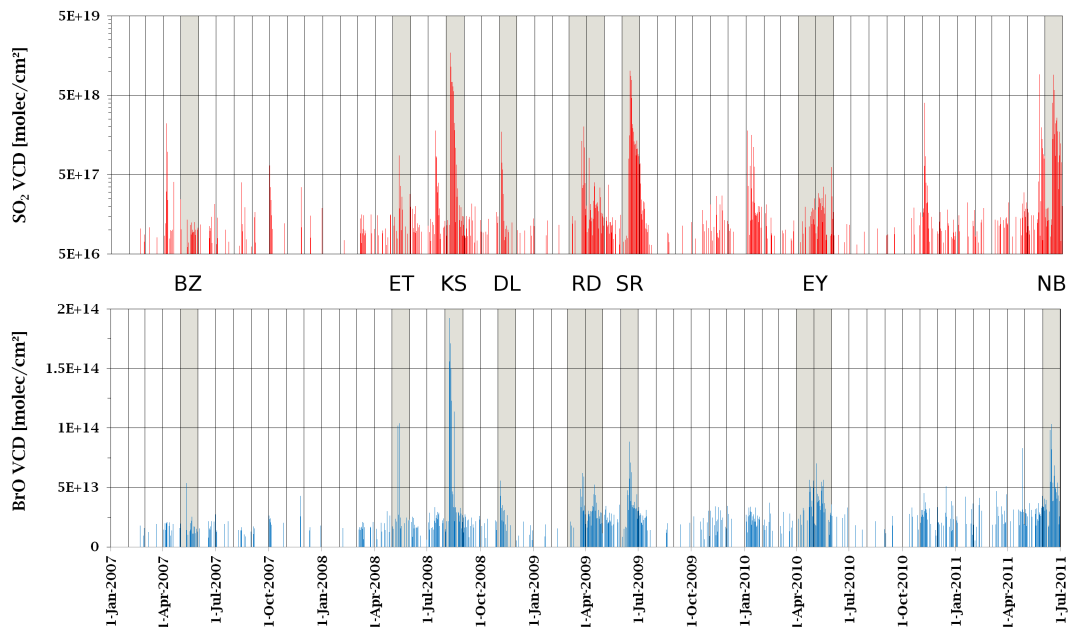


**Fig. 5.** Time-series of maximum GOME-2  $\text{SO}_2$  and BrO VCDs\* (geometrical AMF and background corrected) within all individual volcanic plumes, captured by the automatic plume detection algorithm between January 2007–June 2011. For several  $\text{SO}_2$  plume events, the maximum BrO VCDs\* are significantly elevated at the same time (please note the logarithmic scale for  $\text{SO}_2$ ). This is in particular the case for the eruptions during the highlighted periods (BZ – Bezymianny, ET – Etna, KS – Kasatochi, DL – Dalaffilla, RD – Redoubt, EY – Eyjafjallajökull, NB – Nabro).

[Title Page](#)
[Abstract](#)
[Introduction](#)
[Conclusions](#)
[References](#)
[Tables](#)
[Figures](#)
[◀](#)
[▶](#)
[◀](#)
[▶](#)
[Back](#)
[Close](#)
[Full Screen / Esc](#)
[Printer-friendly Version](#)
[Interactive Discussion](#)

## Systematic investigation of BrO in volcanic plumes with GOME-2

C. Hörmann et al.

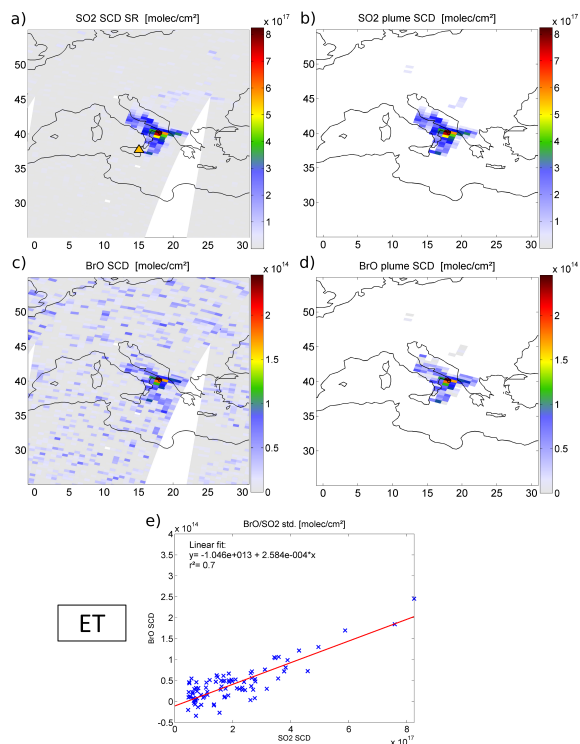


**Fig. 6.** SO<sub>2</sub> and BrO SCDs during an eruptive phase of Mt. Etna on 14 May 2008. The SCDs for SO<sub>2</sub> and BrO (**a** and **c**) show that the BrO SCDs were clearly enhanced in the area of the SO<sub>2</sub> plume and even have a similar distribution. (**b**) and (**d**) show only those satellite pixels, that are supposed to represent the volcanic plume (SO<sub>2</sub> VCD\* > 3σ\*). The correlation plot for the identified plume pixels (**e**) shows a linear relationship between the two species ( $r^2 = 0.7$ ) and a fitted mean BrO/SO<sub>2</sub> ratio of  $\sim 2.5 \times 10^{-4}$ .

Title Page

Abstract

Introduction

Conclusions

References

Tables

Figures

◀

▶

◀

▶

Back

Close

Full Screen / Esc

Printer-friendly Version

Interactive Discussion

## Systematic investigation of BrO in volcanic plumes with GOME-2

C. Hörmann et al.

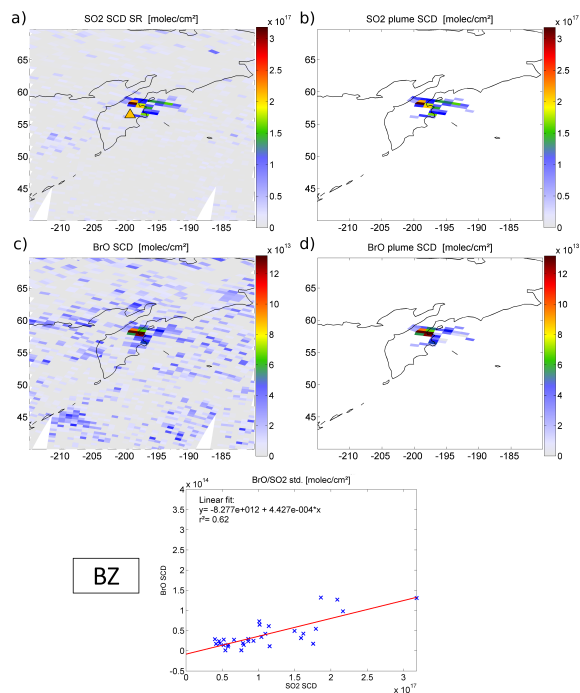


**Fig. 7.**  $\text{SO}_2$  and BrO SCDs during an eruptive phase of Bezymianny volcano (Kamchatka Peninsula) on 11/12 May 2007. Next to the  $\text{SO}_2$  plume (a), volcanic BrO was present, as the BrO SCDs are clearly enhanced in the area of the  $\text{SO}_2$  plume (c). The satellite pixel with  $\text{SO}_2$  SCDs  $> 3\sigma$  of the reference area are shown in (b) and (d) for both species. The correlation plot for the identified plume pixels (e) shows a linear relationship between the two species ( $r^2 = 0.62$ ) and a fitted mean BrO/ $\text{SO}_2$  ratio of  $\sim 4.4 \times 10^{-4}$ .

Title Page

Abstract

Introduction

Conclusions

References

Tables

Figures

⏪

⏩

◀

▶

Back

Close

Full Screen / Esc

Printer-friendly Version

Interactive Discussion

## Systematic investigation of BrO in volcanic plumes with GOME-2

C. Hörmann et al.

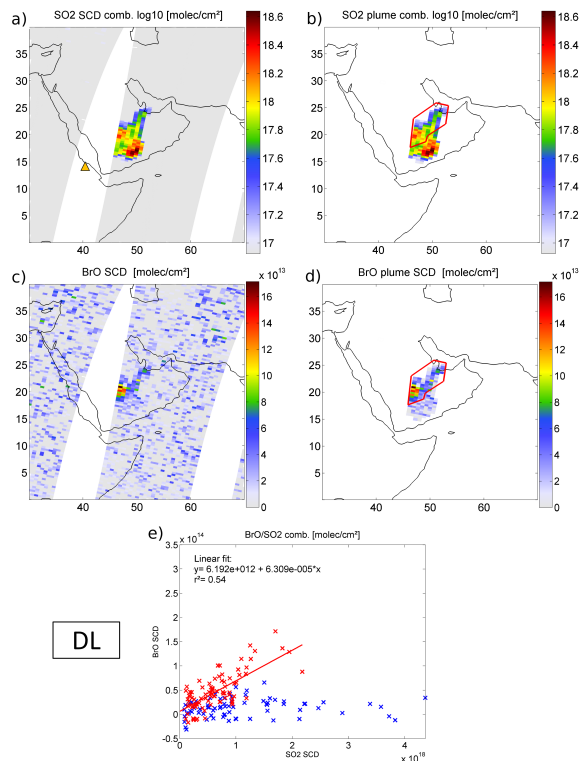


**Fig. 8.** GOME-2 measurements of  $\text{SO}_2$  and BrO SCDs after the eruption of the Dalaffila volcano on 4 November 2008. The  $\text{SO}_2$  plume is separated into two main parts and can be clearly seen in (a) the combined  $\text{SO}_2$  retrieval (please note the logarithmic scale). In (b), only the significantly enhanced  $\text{SO}_2$  SCDs\*  $> 3\sigma^*$  are shown. Enhanced BrO SCDs\* are only located in the north-western part (c and d). A linear correlation can only be seen for a restriction to this area, which is indicated by the red polygon in the maps and the red crosses in the correlation plot (e). Blue crosses represent measurements outside the selected area. The  $r^2$  is then 0.54 with a fitted mean BrO/ $\text{SO}_2$  ratio  $\sim 6.3 \times 10^{-5}$ .

## Systematic investigation of BrO in volcanic plumes with GOME-2

C. Hörmann et al.

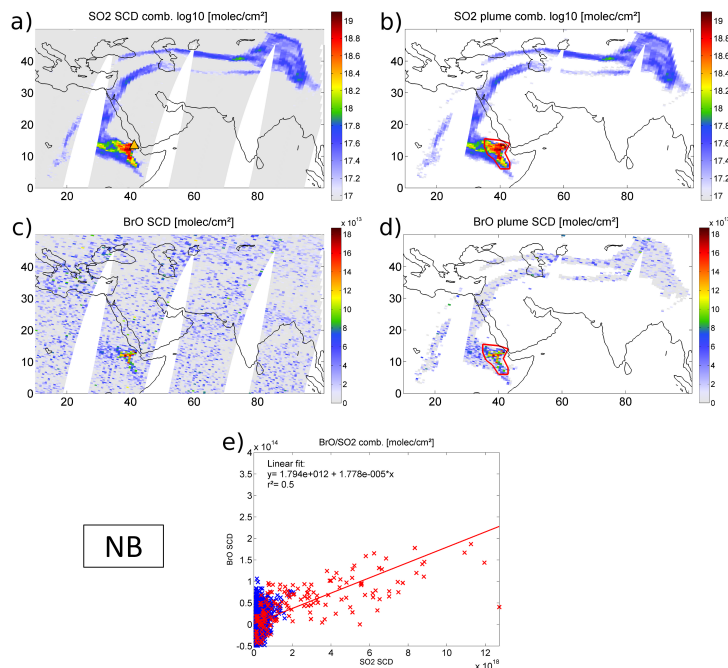


**Fig. 9.** SO<sub>2</sub> and BrO SCDs during the eruption of the Nabro volcano (Eritrea) on 16 June 2011. The SO<sub>2</sub> plume spreads several thousands of kilometres from the volcano towards East Asia (a and b). The enhanced BrO SCDs\* appear only relatively close to the volcano (in the same area where the highest SCDs\* of SO<sub>2</sub> are detected) and show a similar distribution (b and d). While the  $r^2$  from the linear fit for *all* identified plume pixels (blue and red crosses) is rather low (0.29), the restriction to the area with clearly enhanced BrO SCDs\* results in  $r^2 = 0.5$  (area is indicated by the red polygon in (c) and (e); corresponding SCDs\* by red crosses in the correlation plot e). The fitted mean BrO/SO<sub>2</sub> ratio is low compared to other eruptions with  $\sim 1.8 \times 10^{-5}$ .

## Systematic investigation of BrO in volcanic plumes with GOME-2

C. Hörmann et al.

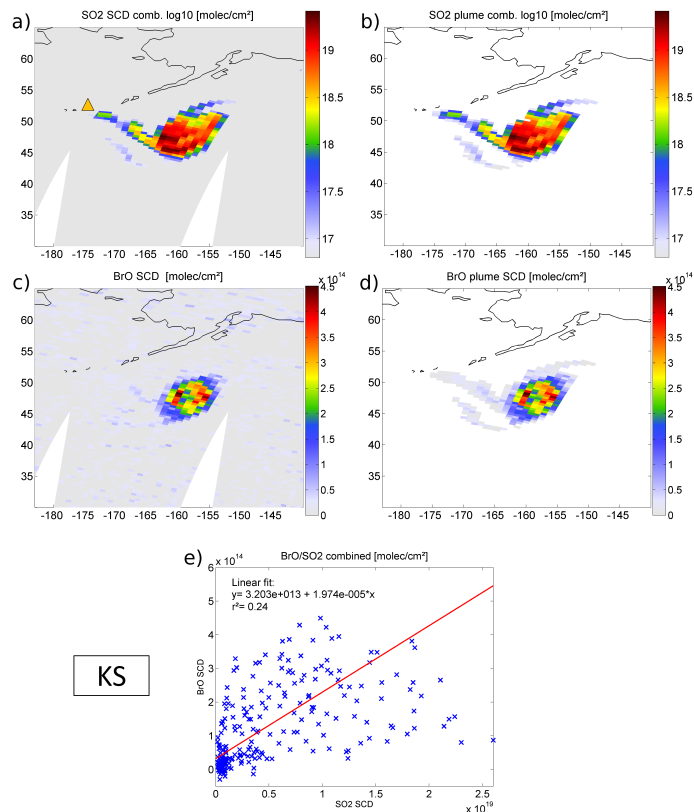


**Fig. 10.** SO<sub>2</sub> and BrO SCDs during the second day of the Kasatochi eruption (9 August 2008). While the SO<sub>2</sub> plume (a and b) and the enhanced BrO (c and d) are in principle located at the same area, the spatial distribution for BrO appears more circular than for the SO<sub>2</sub>. The correlation plot (e) shows a positive correlation between the species ( $r^2 = 0.24$ ), but also a large scatter in the BrO SCDs\* with increasing SO<sub>2</sub> SCDs\*.

Title Page

Abstract

Introduction

Conclusions

References

Tables

Figures

◀

▶

◀

▶

Back

Close

Full Screen / Esc

Printer-friendly Version

Interactive Discussion



## Systematic investigation of BrO in volcanic plumes with GOME-2

C. Hörmann et al.

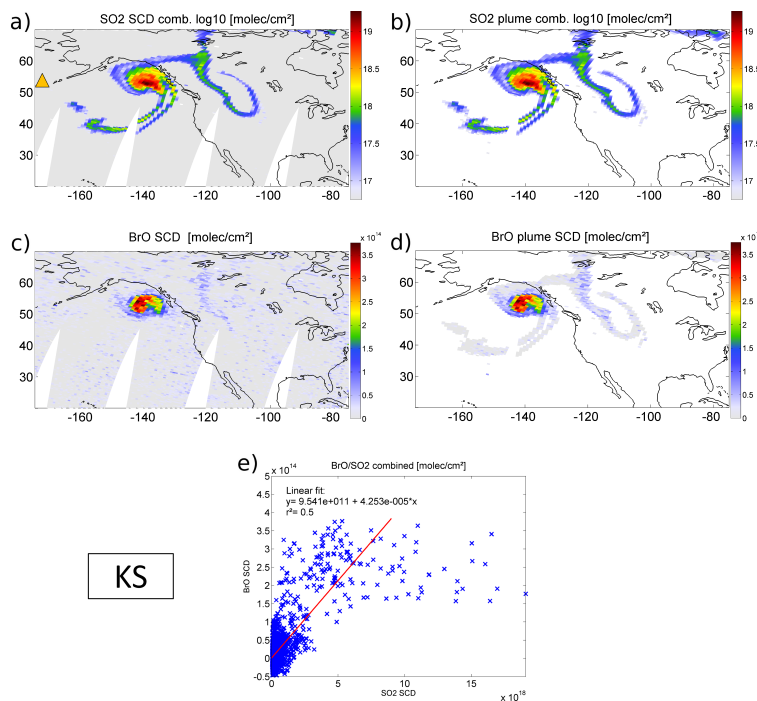


**Fig. 11.** GOME-2 maps for SO<sub>2</sub> and BrO for the volcanic plume of Kasatochi on 11 August 2008. The centre part of the plume has further travelled in eastern direction, several branches now extend from the plume centre in south western and north eastern direction (a and b). The enhanced BrO SCDs\* are located around the centre region, but the distribution inside this area remains different compared to the one for SO<sub>2</sub> (c and d), as the highest SO<sub>2</sub> SCDs\* appear directly in the plume centre, while the BrO seems to be twisted around it. This can also be seen in the correlation plot (e), where the BrO columns are independently scattered around  $2.5 \times 10^{14}$  for SO<sub>2</sub> SCDs\*  $> 5 \times 10^{18}$  molecule cm<sup>-2</sup>.

Title Page

Abstract

Introduction

Conclusions

References

Tables

Figures

◀

▶

◀

▶

Back

Close

Full Screen / Esc

Printer-friendly Version

Interactive Discussion

## Systematic investigation of BrO in volcanic plumes with GOME-2

C. Hörmann et al.

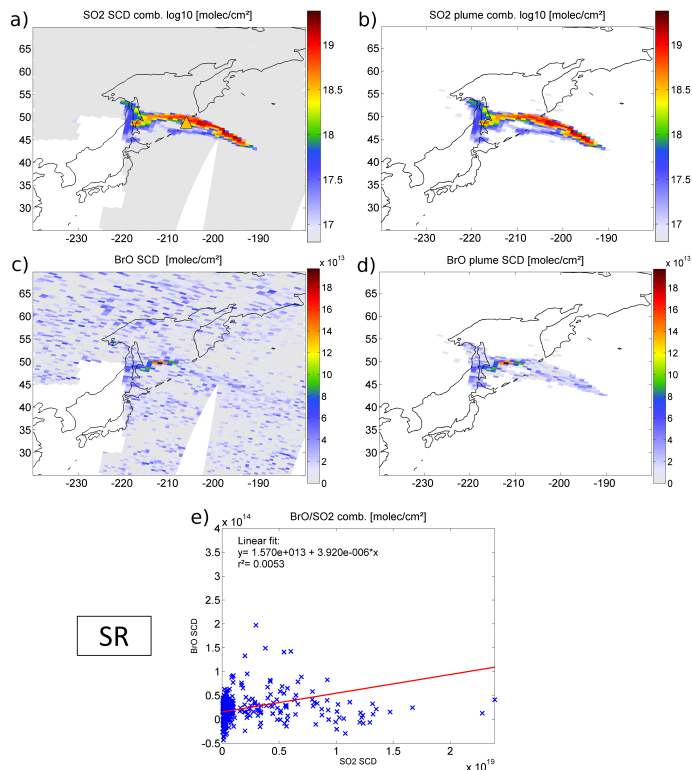


**Fig. 12.** The volcanic  $\text{SO}_2$  and BrO plume during the eruption of Sarychev on 15/16 June 2009. The  $\text{SO}_2$  plume (**a** and **b**) is transported in western and eastern direction from the volcano (indicated by the orange triangle in **a**; the white area in the lower left corner is due to data restrictions in order to prevent the detection of anthropogenic  $\text{SO}_2$  over China). Surprisingly, enhanced BrO columns are only observed in a fraction of the western part (**c** and **d**). The correlation plot for both species therefore lead to an  $r^2$  value close to zero from the bivariate linear fit (**e**).

Title Page

Abstract

Introduction

Conclusions

References

Tables

Figures

◀

▶

◀

▶

Back

Close

Full Screen / Esc

Printer-friendly Version

Interactive Discussion

## Systematic investigation of BrO in volcanic plumes with GOME-2

C. Hörmann et al.

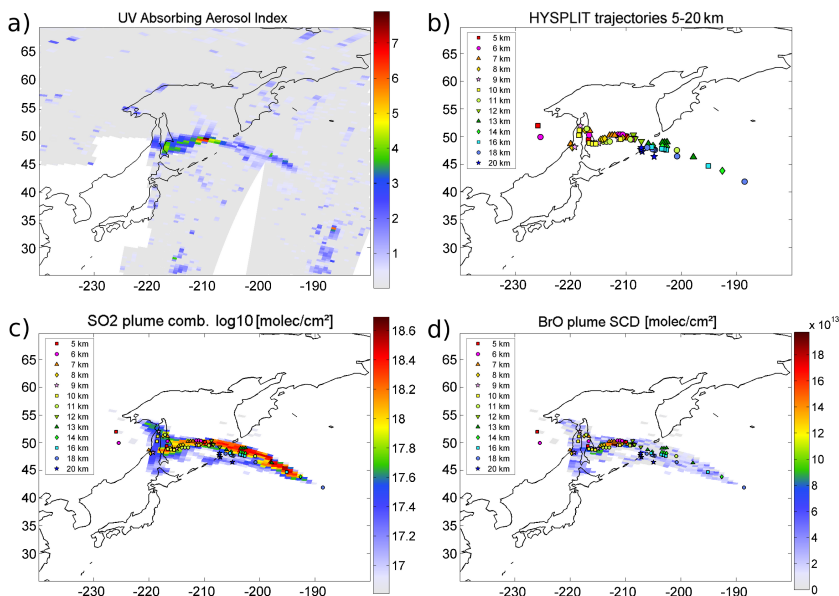


**Fig. 13.** (a) UV Absorbing Aerosol Index (AAI) for the Sarychev eruption on 15/16 June 2009. Like for BrO, the highest values occur in the western part of the plume, indicating an ash-rich explosion in temporal proximity to the satellite measurements. (b) HYSPLIT trajectory end-points for starting heights between 5 and 20 km of the last 5 major explosions during the two days before the GOME-2 measurements took place. The trajectory simulations point out, that the wind changed from western to eastern direction between 11 and 13 km with increasing height. (c) Overlap of the volcanic SO<sub>2</sub> plume from the combined retrieval with the trajectory end-points. (d) Overlap of the BrO<sub>2</sub> SCDs\* in the area of the captured SO<sub>2</sub> plume with the trajectory end-points.

[Title Page](#)
[Abstract](#)
[Introduction](#)
[Conclusions](#)
[References](#)
[Tables](#)
[Figures](#)
[◀](#)
[▶](#)
[◀](#)
[▶](#)
[Back](#)
[Close](#)
[Full Screen / Esc](#)
[Printer-friendly Version](#)
[Interactive Discussion](#)

## Systematic investigation of BrO in volcanic plumes with GOME-2

C. Hörmann et al.

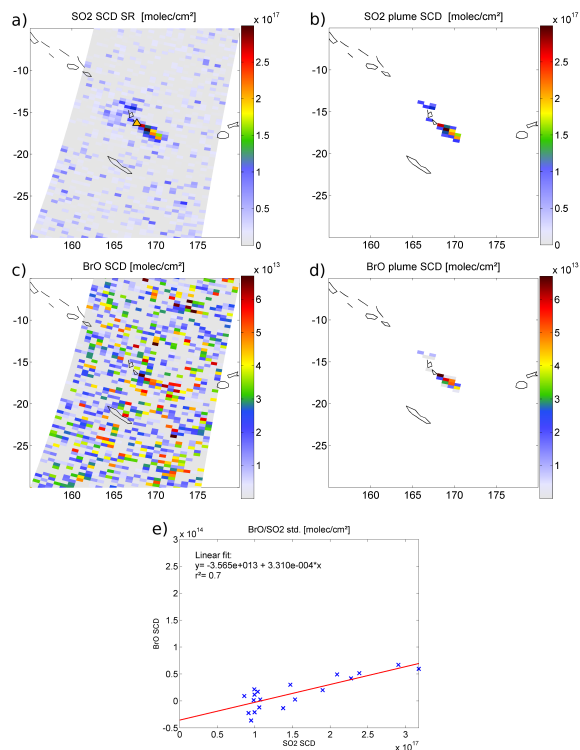


**Fig. 14.** SO<sub>2</sub> and BrO SCDs during a phase of enhanced passively degassing from the Ambrym volcano on 8 April 2010. While the SO<sub>2</sub> plume can be clearly seen in the satellite data (a), enhanced BrO columns are not observed at first sight, since the large scatter indicates values around the instrument's detection limit (c). By focusing on the area of extracted SO<sub>2</sub> plume pixels (b and d), the correlation plot for both species shows a surprisingly clear linear correlation with a resulting  $r^2 = 0.7$  and a relatively high mean BrO/SO<sub>2</sub> ratio of  $3.3 \times 10^{-4}$  from the bivariate linear fit (e).

Title Page

Abstract

Introduction

Conclusions

References

Tables

Figures

◀

▶

◀

▶

Back

Close

Full Screen / Esc

Printer-friendly Version

Interactive Discussion

## Systematic investigation of BrO in volcanic plumes with GOME-2

C. Hörmann et al.

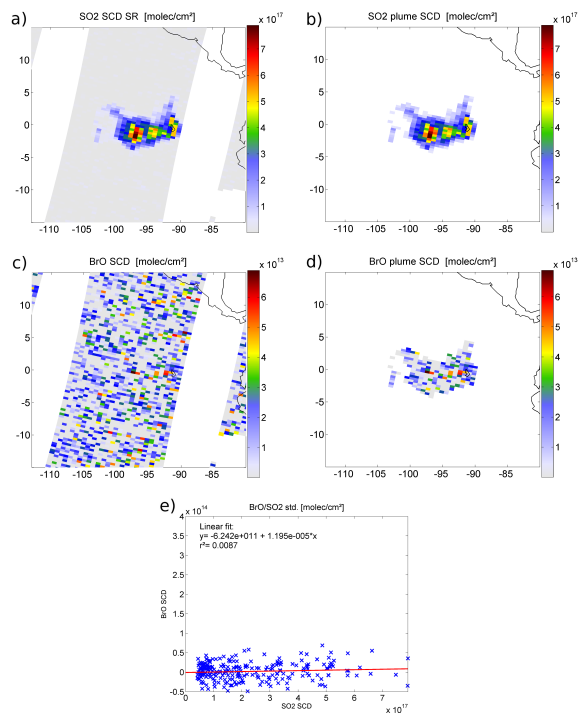


**Fig. 15.** SO<sub>2</sub> and BrO SCDs for the eruption of the Fernandina volcano (Galapagos Islands, Ecuador) on 13 April 2009. The background corrected SCDs\* for SO<sub>2</sub> and BrO are shown (a and c), including the pixels of the PEB and the reference area. Accordingly, the extracted plume pixels are shown in (b) and (d). The resulting correlation plot (e) shows no correlation between the two species as for the majority of all investigated plumes. The BrO SCDs\* are statistically distributed over the whole area of the volcanic SO<sub>2</sub> plume, resulting in a vanishing correlation and a BrO/SO<sub>2</sub> ratio close to zero.